CALIFORNIA STATE UNIVERSITY, NORTHRIDGE

GEOLOGY AND GEOMORPHOLOGY OF THE INTERSECTING MISSION CREEK AND BANNING FAULT STRANDS, SOUTHERN SAN ANDREAS FAULT

A thesis submitted in partial fulfillment of the requirements
for the degree of Master of Science
in Geology

By

Nathan E. Guzman

May 2010

The thesis of Nathan E. Guzman is approved:

Richard Heermance, Ph.D.	Date
Elena Miranda, Ph.D.	Date
J. Douglas Yule, Ph.D. (Chair)	Date

California State University, Northridge

DEDICATION

To my wonderful parents Eduardo and Linda Guzman, for all of your love and encouragement through the years and always pushing me to try my best. To all of my family, to those who are with us and those whom are not, thank you for your support and love growing up. And, to my wonderful girlfriend Wyndee Haley, thank you for your love and providing me with inspiration to write.

ACKNOWLEDGEMENTS

I gratefully thank Sterling Wainscott and Wade Malone of Granite Construction Co. for allowing me access onto quarry property. Fieldwork for this study was funded by the 'Catalyst Program' at CSUN (NSF-GEO-0503609). Thank you to the 'Catalyst Program' for inspiring me to become a graduate student, and especially to Drs. Kathie Marsaglia, Doug Yule, Gerry Simila and Vicki Pedone, whom initiated the program and dedicated many hours to keep it running smoothly.

I am much obliged for the help Whitney Behr provided and sharing her knowledge and wisdom regarding the complexities of Biskra Palms. I would also like to thank Dr. Ray Weldon and his earthquake geology class at UCLA for their much-appreciated help in the preparation of the excavation walls. For spending long hours in the Indio sun, trench logging and surveying, I thank Cristo Ramirez, Chris Forester, Noel Velasco and Wyndee Haley. I appreciate the help of Ken Hudnut and Ray Weldon for their judgment in placing the excavation locations.

I graciously thank my advisor Dr. Doug Yule for his patience, insights and extensive knowledge of the field. I very much appreciate your friendship and willingness to teach and guide me as I completed this thesis. I also could not have finished this thesis without the last minute stipends you thoughtfully provided me with. I thank my committee members Drs. Richard Heermance and Elena Miranda for their constructive criticism in editing this thesis.

Lastly, I would like to thank my loving parents Eduardo and Linda Guzman for their never-ending encouragement in pursuing my education, as well as my younger brother and sister, Nicholas and Lauren Guzman for being supportive and loving. Finally, I would like to thank my wonderful girlfriend Wyndee Haley, whom helped me greatly with much encouragement and love in the trials of completing this thesis.

TABLE OF CONTENTS

LIST OF ILLUSTRATIONS

LIST OF TABLES

LIST OF PLATES

ABSTRACT

GEOLOGY AND GEOMORPHOLOGY OF THE INTERSECTING MISSION CREEK AND BANNING FAULT STRANDS, SOUTHERN SAN ANDREAS FAULT

By

Nathan E. Guzman

Master of Science in Geology

The Mission Creek and Banning strands of the San Andreas fault zone merge at Biskra Palms, near Indio, CA. Here faulting appears to have dextrally displaced the northern margin of an ~50 ka alluvial fan by ~600 to 700 m in a right-lateral sense. Some geologic maps however, show a thrust fault that merges with the downstream edge of the fan and raises the possibility that the fan edge has been structurally modified since abandonment. We excavated a series of cuts across the fan edge to test this hypothesis. These cuts reveal features that support a thrust fault model as they show a 1-m-thick, sub-horizontal shear zone that contains Plio-Pleistocene Palm Spring Formation in its hanging wall and late Pleistocene alluvium and Holocene(?) colluvium and alluvium in its footwall. The excavations clearly show that the shear zone overrides paleo-topography of the ~50 ka fan. In places colluvium and alluvium fill low-lying areas ahead of the hanging wall block that was subsequently

overridden by motion on the thrust. Faulting therefore post-dates the youngest footwall unit. Though no dateable material has been obtained, the unconsolidated nature and lack of soil development suggest that the colluvium and alluvium found in the footwall is quite young. Several features support a SE-transport direction of the fault including map-scale E-W trending open folds in the hanging wall and SE-trending slickenlines within the shear zone. In addition, the hanging wall block contains alluvial strath terraces that are cut into the Palm Spring Formation, ~30-50 m above the footwall. Though their age is unknown, the soil and desert varnish on terrace boulders resembles the ~50 ka fan surface in the footwall. This possible correlation yields an uplift rate of 0.5-1.0 mm/yr, and slip rate of 1-2 mm/yr assuming a 30-degree dipping thrust and a San Andreas-parallel slip vector. The margin of the ~50 ka fan is therefore substantially modified by thrust faulting and using the fan edge to constrain displacement would underestimate the total amount of right-lateral slip across the San Andreas fault here. Our new model interprets the thrust as the surface trace of the Banning fault strand where it overrides the Biskra Palms fan and merges with Mission Creek fault strand.

INTRODUCTION

Obtaining slip rates along the southern San Andreas fault is critical to help assess the seismic hazard in southern California. The next major rupture is likely to occur here and poses a major threat to southern Californians (Sieh, 1985; Sieh and Williams, 1990; Burciaga et al., 2004; Philibosian et al., 2009). Accurate slip rates assist in estimating potential rupture zones and recurrence intervals. For the Coachella Valley segment of the San Andreas fault (Figure 1), it has been estimated that five large events have occurred since A.D. 825, with the most recent in A.D. 1520-1680 (Fumal et al., 2002). An average recurrence interval for these events is estimated at 215 ± 25 years (Fumal et al., 2002). Being that approximately more than 300 years have elapsed since the last rupture this segment of the San Andreas fault appears to be overdue for failure (Fumal et al., 2002; Weldon et al., 2004). Thus, the southern segment poses major a threat to infrastructure and southern California residents as it is assumed an event here would produce a > M7.0 magnitude earthquake and rupture nearly 200 km length of the fault (Fumal et al., 2002; Jones et al., 2008).

The two most active fault zones in southern California lie to the west and northwest of the Coachella Valley San Andreas fault (CVSAF), the San Jacinto fault and Eastern California Shear Zone (ESCZ), respectively (Bennett et al., 1996; Dorsey et al., 2002). The lack of slip on the CVSAF is used by some to suggest that the CV region is the most likely source for the next 'Big One' in southern California (Fumal et al., 2002; Jones et al., 2008). The latter is employed by others to argue that the CV segment is being bypassed by more

active faults systems to the east and west (Dokka and Travis, 1990; Dolan et al., 2007).

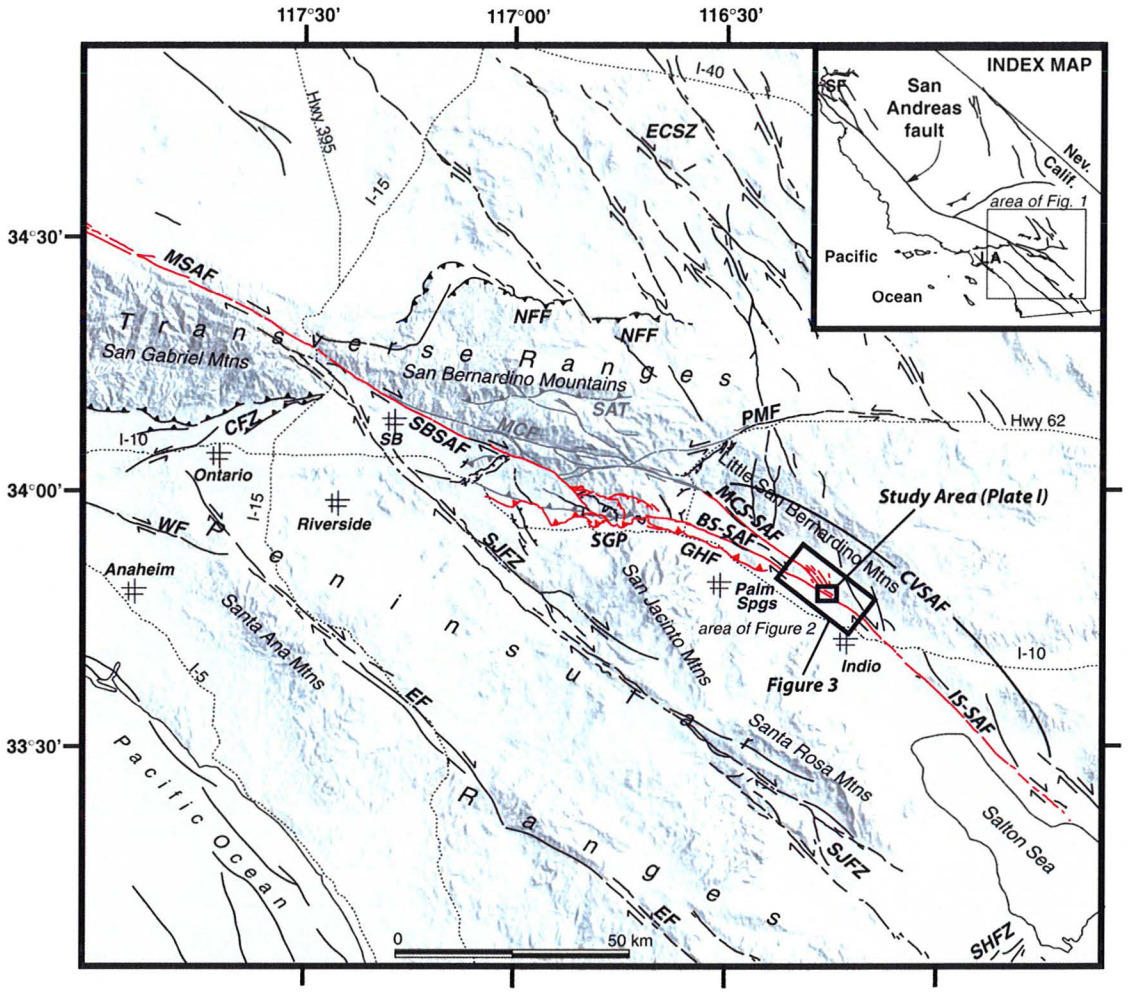

Figure 1. Generalized shaded relief map of southern California, depicting the major faults of the region. The main strands of the San Andreas fault are shown in red. Other active faults are shown in black; inactive faults in gray. The study area is located at the intersection of the Banning and Mission Creek strands of the San Andreas fault. Abbreviations: CFZ, Cucamonga fault zone; CHFZ, Crafton Hills fault zone; BS-SAF, Banning strand San Andreas fault; MCS-SAF, Mission Creek San Andreas fault; EF, Elsinore fault; ECSZ, eastern California shear zone; GHF, Garnet Hill fault; IS-SAF, Indio Strand San Andreas fault; MCF, Mill Creek fault; MSAF, Mojave segment, San Andreas fault; NFF, north frontal fault; PMF, Pinto Mountain fault; SAT, Santa Ana thrust; SBSAF, San Bernardino strand, San Andreas fault; SGPFZ, San Gorgonio Pass fault zone; SHFZ, Superstition Hills fault zone; SJFZ, San Jacinto fault zone; and WF, Whittier fault. Map modified from Yule & Sieh, 2003.

The San Jacinto fault is the most seismically active fault in southern California and the ECSZ has had the largest earthquakes in California since 1952 (1992 M7.3 Landers and 1999 M7.1 Hector Mine earthquakes).

An offset late Pleistocene fan southeast of Biskra Palms oasis is an ideal place to evaluate the slip rate of the southern San Andreas fault. A series of excavations were made at the northern end of the lower fan surface, labeled as T2d by van der Woerd et al. (2006). These exposures revealed that the fan surface is truncated by a low-angle shear zone with Plio-Pleistocene sediments in the hanging wall. This poses the problem of accurately locating the fan margin, used by previous researchers as a piercing line to reconstruct slip across the Coachella Valley Mission Creek strand (Keller et al., 1982; van der Woerd et al., 2006). Relations exposed in the trenches show that the fan margin is overridden, but poses a new question of what is cause of this truncation. This is explored in two hypotheses shown in Figure 2 1) the northern edge of T2d is a depositional edge where the Palm Spring Formation forms a buttress unconformity with the Biskra fan or 2) Palm Spring Formation overrides the northern edge of the Biskra fan, concealing its true edge. My findings support the former hypothesis in which the Banning fault acts as a thrust fault as it forms a compressional stepover as it merges with the Mission Creek strand.

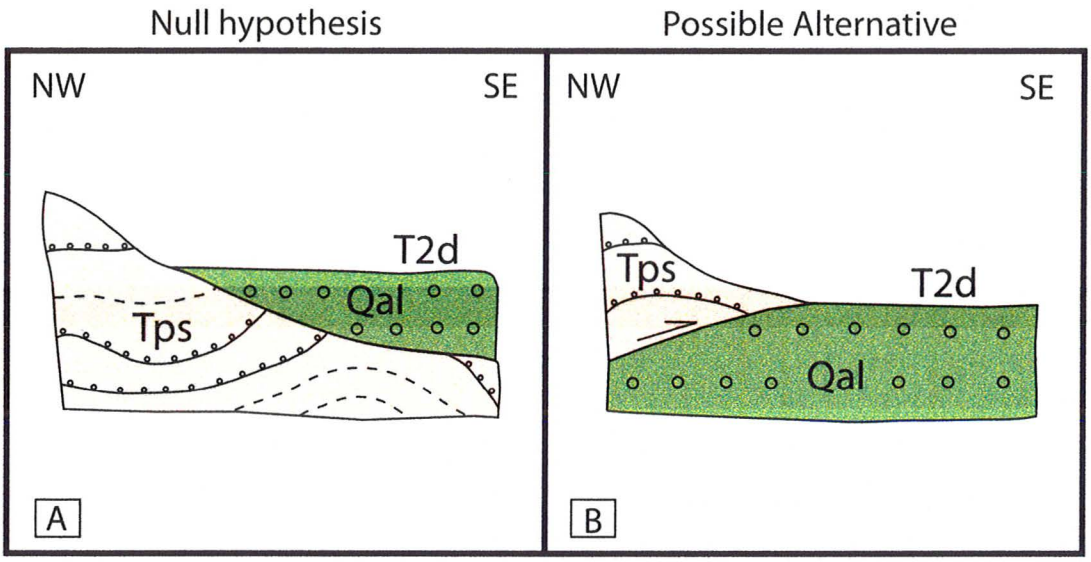

Figure 2. Schematic cross-sections showing competing hypotheses for margin of the T2d alluvial fan. A) T2d alluvial fan onlaps onto exposure of Palm Spring Fm.; contact between T2d surface and Tps formed when fan deposition ceased. B) T2d alluvial fan overridden by thrust fault or landslide carrying Palm Spring Fm. in its hanging wall.

GEOLOGIC SETTING

The study area is located in the southern Big-Bend region of the San Andreas fault, where the Coachella Valley segment of the San Andreas fault consists of a series of strike-slip faults (Figure 1). A broad zone of faulting on the NW that contains several active strands coalesces into a more narrow zone on the SE, and the strike of the faults change from ~N55°W to ~N45°W. I adopted the hierarchical naming scheme of Behr et al. (in press) of segment, strand and splay to describe the faults. The CVSAF segment extends from San Gorgonio Pass to the Salton Sea and consists of four main fault strands, the Garnet Hill fault (GHF) and Banning (BS-SAF), Mission Creek (MCS-SAF), and Indio (IS-SAF) strands (Figure 1).

The study area marks several important structural and tectonic transitions along the CVSAF. The area to the north is characterized by transpression-dominated tectonics whereas the area to the south is characterized by transtension-dominated tectonics. Where the transition from transpressional to transtensional setting occurs, the BS-SAF, MCS-SAF and IS-SAF merge (Figure 1 and Figure 3).

The Indio Hills are located between the MCS-SAF and BS-SAF, and expose Plio-Pleistocene non-marine fluvial sands and gravels of the Palm Spring Formation (Norris & Webb, 1976; Behr et al., in press) and Pleistocene sandstone and fanglomerates of the Ocotillo Formation (Keller et al., 1982) (Figure 3). Most of the Indio Hills are underlain by fanglomerates of the late

Pliocene-Pleistocene Ocotillo Fm (Dibblee, 1954). Canyons and deep gullies expose Pliocene sandstones of the Palm Spring Fm. Lateral facies equivalents of

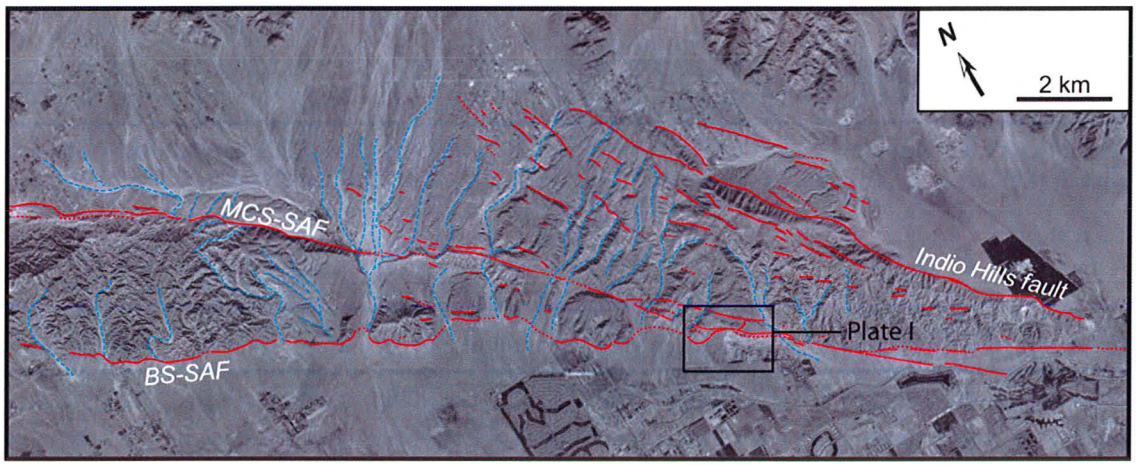

Figure 3. Aerial photograph of the southeastern Indio Hills. Faults are outlined in red and large drainages are outlined in blue. Inferred or buried fault segments are dashed. The intersection of the Mission Creek (MCS-SAF) and Banning strand (BS-SAF) of the San Andreas fault are located within the study area. Modified from Behr et al. (in press).

the Palm Spring Formation include lacustrine deposits of the Borrego Formation and breccias of the Canebrake Formation (Dibblee, 1954; Steely et al., 2009). These non-marine units filled a basin that formed in response to the evolution of the Pacific-North American plate boundary in southern California and northern Mexico (Blake Jr. et al., 1978; Brothers et al., 2009; Steely et al., 2009). Offset stream channels, sags, pressure ridges and abandoned alluvial fans are characteristic of the Indio Hills (Keller et al., 1982). At the northern edge of the Coachella Valley near Indio, the MCS-SAF and BS-SAF uplift the Indio Hills and deform strata of the Plio-Pleistocene Palm Spring Formation, (Norris and Webb, 1976, Behr et al., in press), as well as Ocotillo Formation sandstone and fanglomerates (Keller et al., 1982, van der Woerd et al., 2006).

Located at the mouth of a small canyon the Biskra Palms Oasis is an area within the Indio Hills, where one splay of the MCS-SAF has created an impervious barrier to groundwater and a shallow water table. Southeast of the oasis the BS-SAF and splays of the MCS-SAF cut and uplift a late Pleistocene pediment fan complex into pieces via oblique right-lateral strike-slip movement (Keller et al., 1982; van der Woerd et al., 2006; Behr et al., in press; and Fletcher et al., in press) (Plate I). The splays of the MCS-SAF are approximately 400 m apart and are denoted as NE and SW splays by van der Woerd et al. (2006). The SW Mission Creek splay here is locally delineated by a row of native California Palms (*Washingtonia filiera*) (Keller et al., 1982). The fan complex, referred to as the Biskra fan, has been deformed and uplifted by secondary faulting. This has resulted in the development of fault-related landforms such as beheaded/deflected streams, fault scarps, sagpond deposits and a vertical offset of ~50 m from the lower and intermediated fan surfaces (Keller et al., 1982; van der Woerd et al., 2006; Behr et al., in press). This prominent fan surface is characterized by moderate desert varnish on cobbles and small to rare large boulders with interspersed sandy-pebble desert pavement (van der Woerd et al., 2006). Faulted pieces of the Biskra fan have been labeled T2u, T2i and T2d by van der Woerd et al. (2006), referring to the upstream, intermediate and downstream fan segments. In this thesis I adopt the same nomenclature. Other terrace levels include T3, the oldest alluvial surface at this site, dated at 66 ka by Behr et al. (in press) of which only a small remnant remains between the two splays of the MCS-SAF. Presently, the Biskra fan is the site of an active sand

and gravel quarry owned by the Granite Construction Company. Southeast of the SW Mission Creek splay quarrying operations have removed the modern alluvial wash (T0), which consists of granitic and gneissic cobbles and small boulders in a gravel matrix (Behr et al., in press). The preservation of the next youngest alluvial surface, T1 has also been excavated and once bounded the southeastern edge of T2d (Keller et al., 1982) (Plate I).

PREVIOUS WORK

Keller et al. (1982) published the first slip rate estimate for the CVSAF at the Biskra Palms site. Their slip rate of 10-35 mm/yr is based on a soil age of 20,000 to 70,000 yrs and an ~700 m offset of the alluvial fan margin. Due to the thin veneer of alluvial deposits, they classified the surface as a pediment-fan complex overlying the Ocotillo Formation, although lithologies suggest the Palm Spring Formation underlies the Biskra fan. In the subsurface Keller et al. (1982) classified reddish clay-rich argillic B-horizon paleosols that characterize the Biskra fan. These horizons were used to identify the extent of the fan. Only the upper and lower pieces of the fan were restored for an offset measurement for this study with the middle piece ignored.

Subsequent work by van der Woerd et al. (2006) gives a slip rate of 15.9 ± 3.4 mm/yr based on ^{10}Be and ^{26}Al ages from cobbles of ~35,000 yrs at Biskra Palms and an ~565 m offset of the fan margin. Offset was restored across the NE and SW splays of the MCS-SAF, arguing little or no structural modification of the fan edge since abandonment. Stating that erosion plays a major role in producing uncertainties in surface dating, they sampled only quartz-rich cobbles rooted in the fan surface, avoiding large boulders. They argue that since the cobbles on the T2 surface resemble those in the modern channels, no significant erosion has occurred. Although they indicate the fan surface is developed with a mature pavement, this indicates overall surface deflation and thus significant erosion post abandonment.

Behr et al. (in press) and Fletcher et al. (in press) have recently completed studies that give a slip rate of 17 ± 5 mm/yr based on ^{10}Be and ^{26}Al ages from boulders and U-series soil ages, respectively, and a ~770 m offset of the alluvial fan's axis. They describe the surface as containing patches of moderate desert pavement with indications that the surface has deflated due to wind erosion by the presence of stacked cobbles and boulders. Swales on the T2u and T2i surfaces indicate that minor faulting has caused significant modification of the original surface. Behr et al. (in press) also distinguishes an older surface (T3i) based on a more well developed desert pavement. The cosmogenic radionuclide age of T3i is 66 ± 6.0 ka. Using a revised approach, Behr et al. (in press) applied the cosmogenic method to date the Biskra fan. Behr et al. (in press) sampled only tops of m-size boulders protruding from the fan surface, due to the higher probability of inheritance or re-exposure to sunlight due to movement before burial associated with cobbles. The chances for inheritance errors are greater for cobbles, thus reducing the accuracy in obtaining sound age data (Matmon et al., 2005). Of the unlikely chance that a large boulder would be redeposited in the same orientation, it is assumed the likeliness for inheritance is minor. ^{10}Be isotopic ages by Behr et al. (in press) yield a fan 45-56 ka surface age. The lack of datable material in arid to semiarid environments limits the dating techniques that can be used.

Fletcher et al. (in press) used an alternate technique; sampling U-Th concentrations from pedogenic carbonate rinds at the Biskra fan site. Samples were taken in the calcic horizon located within the paleosol of the T2 surface.

Multiple samples were taken from pits excavated on all sections of the fan. Developed on the undersides of cobbles as rinds during pedogenesis, pedogenic calcium carbonate accumulates from older eroded fragments of calcium carbonate and is deposited as parent material (Ku et al., 1979). The abundance of calcium carbonate within the paleosols and multiple collection sites gave Fletcher et al. (in press) several ages to quantify, ultimately yielding a minimum age of 45.1 ± 0.6 ka, fitting well with results from Behr et al. (in press). This further supports a fan surface age of 45-50 ka, and indicates the lessening chance for inheritance errors when sampling boulder tops. This age also argues for significant deflation of the fan surface post abandonment.

Behr et al. (in press) abandons use of the fan edge as an offset marker because of significant structural modification (This Study). Thus, they used the fan's central axis as defined by maximum curvature of topographic lines as an offset marker; ironically, the results of the Behr et al. (in press) and Fletcher et al. (in press) papers yield a similar rate to van der Woerd et al. (2006) but with more robust age and offset data.

Slip rates appear to slow from ~25 mm/yr at Cajon Pass to <10 mm/yr at San Gorgonio Pass and increase to ~20 mm/yr in the Coachella Valley. Paleoseismology studies obtain slip rates through the analysis of single fault strands in a system of faults, thus these estimates are considered minimum rates. Slip rates provided by geodetic studies are model driven and most only utilize single fault strand, simple geometry fault models for the San Gorgonio Pass. Simple models have been shown to underestimate slip rates in the SGP region

(Dair and Cooke, 2009). The lowering of slip rates at SGP may be due to transfer of slip off the SAF and onto the San Jacinto fault and/or the ECSZ (Matti et al., 1993; Kendrick et al., 2002; Yule and Sieh, 2003; Meade and Hager, 2005).

Published slip rates for the CVSAF average ~20 mm/yr, but geodetic models give a slightly higher average rate (22 mm/yr) than geologic studies (~16 mm/yr) (Table 1). An outlier on this table, the slip rate of 4 mm/yr is from a paleoseismic site on the CVSAF at Thousand Palms oasis where slip is dying out toward the NW. Most slip on the San Andreas is carried by the BS-SAF at this latitude, so the 4 mm/yr slip rate represents about 20% of the total CVSAF rate. Geologically determined slip rates provide slip from specific faults being studied, thus giving a more refined slip rate on a single fault and may miss off-fault deformation. The more general measurements of GPS data allows for recording of slip across a fault zone, thus geologic rates must be considered minimum values.

Table 1. Slip rate estimates for the southern San Andreas fault.

Reference	Model type	Slip Rate (mm/yr)
	Entire sSAF	
Fialko et al. (2005)	INSAR	25 ± 3
	sSAF—San Bernardino segment	
Bennett et al. (1996)	GPS—elastic block model	26 ± 2
Meade and Hager (2005)	GPS—elastic block model	5.1 ± 1.5
Becker et al. (2005)	GPS and stress inversions	-2.0 ± 15
Weldon and Sieh (1985)	Geology—offset feature	24 ± 3.5
Harden and Matti (1989)	Geology—offset feature	14 - 25
McGill et al. (2007)	Geology—offset feature	14 ± 3
	Coachella Valley segment	
Bennett et al. (1996)	GPS—elastic block model	22 ± 2
Becker et al. (2005)	GPS and stress inversions	23.0 ± 8
Meade and Hager (2005)	GPS—elastic block model	23.3 ± 0.5
Fay and Humphreys (2005)	GPS—elastic and viscoelastic finite element	22.3 ± 0.7
Bennett et al. (2008)	GPS—elastic block model	6.7 – 10.7
Keller et al. (1982)	Geology—offset alluvial fan	10 – 35
Dorsey (2003)	"	15 ± 3
van der Woerd et al. (2006)	"	15.9 ± 3.4
Behr et al. (in press)	"	12.0 – 21.7
Fumal et al. (2002)	Geology—paleoseismology	4 ± 2
	sSAF—Banning/ San Gorgonio Pass	
Orozco (2004)	Geology—paleoseismology	5-10
Yule (unpublished data)	Geology—offset alluvial gravels	5-6
	Transfer from sSAF onto ECSZ	
Meade and Hager (2005)	Eureka Peak fault	21.3 ± 1.6

(Table modified from Behr et al., in press)

METHODS

I conducted fieldwork in the fall and summer of 2008, and completed mapping in summer of 2009. The Biskra fan is actively being quarried and permission to access the site was generously granted by Granite Construction Company.

A track-hoe and operator provided by S&L Equipment (Corona, Ca) opened a series of excavations. The excavation walls were cleaned and a 1 x 1 m string grid was used to form a reference grid. Each excavation was photographed individually in low-sunlight conditions to make a photo mosaic used as a base for logging. Photos were stitched together using Adobe Photoshop®. Various observations were noted while logging including grain size using the Wentworth grain size chart, bedding features, color, clast size and identification of shear planes and fault-induced structures. Orientations of shear planes and other features were measured when possible. Using the photomosaics, logs were drawn and digitally colored using Adobe Illustrator®, allowing for units and features seen in the excavations to be identified clearly.

A high-resolution digital image was produced from USGS B4 LiDAR imagery set (Plate I) and was generated with the use of the QT Modeler program (by Applied Imagery). Sun angles were optimally adjusted to accentuate the topography on this image. Topographic profiles were generated by drawing lines of section on the LiDAR image using QT modeler that yielded m-scale resolution for the topographic profiles.

GEOLOGIC UNITS

Palm Spring Formation (Pliocene)

The base and top of this unit is not exposed, however exposed units range about ~200 m in thickness. Beds generally dip <20° and contain open folds that trend E-W. The formation is poorly exposed in steep gullies and canyons, but is also exposed in the trenches. These beds consist of alluvial/non-marine fluvial conglomerates, sandstones, siltstones and mudstones in approximately the following percentages 10/70/10/10% (Dibblee, 1954; Norris and Webb, 1976; Keller et al., 1982; Lutz et al., 2006; Behr et al., in press).

Massively to thin tabular beds are common. Locally, beds are lenticular with sharp contacts and local scours. The unit is generally structureless, but cross-stratification in sands locally occurs and graded beds in conglomerate also are locally observed. Sand and gravel exposures are locally quite friable, but overall outcrops are well indurated.

Ocotillo Formation (Plio-Pleistocene)

I did not observe this unit in outcrop, but this unit forms a low-relief upland surface overlaying the Palm Spring Fm. (Plate I). A poorly developed pavement of coarse gravel and common m-scale boulders characterizes this surface. Compositions of clasts include granitic rocks and quartzo-feldspathic gneiss with rare mica schist. The contact with the underlying Palm Spring Fm. may be parallel to bedding, hence the lack of large boulders in the Palms Spring units.

Quaternary Alluvial Fan Deposits

These alluvial fan deposits are exposed only in trench excavations. Beds have a <5°dip, with the exception of T2i, which has been modified by backtilting and a dip of ~22° to the NE (Behr et al., in press) (Plate I).

The total thickness of alluvial units is unknown, however, ~80 m of alluvium has been exposed in the Granite Construction Company quarry exposing alluvial deposits beneath the T2d subsurface. Beds are uniform in structure and well stratified. The alluvium consists of loosely consolidated fine to coarse sands and gravels with well-developed paleosols common for most surfaces.

ALLUVIAL FAN SURFACES

A number of alluvial fan surfaces are recognized based on relative development of soils and desert varnished pavement (Keller et al., 1982). There are three distinct surfaces present of which two have been removed completely by quarrying. The alluvial surfaces can be discerned according to the amount of varnish as well as the soil maturity. All rills and gullies on these surfaces slope to southwest.

T0

These are the modern alluvial surfaces, which drain off the Indio Hills. Subsurface units are not exposed in outcrop. Clasts consist of mainly granitic pebbles and cobbles that are possibly sourced from the Little San Bernardino Mountains; no m-size boulders were observed.

T1

Mapped by van der Woerd et al. (2006) using air photos, this surface is considerably lighter in color than T2 and T3. This is perhaps due to fewer percentages of surface cobbles and boulders containing varnish, which indicates a younger surface. This portion of the fan was quarried and destroyed prior to 2000 (van der Woerd et al., 2006). It was noted by van der Woerd et al. (2006) that the air photos indicated this surface was lower topographically to T2 and appeared to have fewer rills or swales cutting the alluvium.

T2

The T2 surface is the most prominent at Biskra Palms and is the focus for obtaining slip rates along the southern SAF (Keller et al., 1982; van der Woerd et

al., 2006; Behr et al., in press; Fletcher et al., in press). The broad zone of deposition and shallow dip of the fan surface indicate that T2 was deposited during times of intermittent precipitation that is specific to semiarid to arid regions (Blissenbach, 1954). Other indicators of infrequent but intense rainfall include the presence of very large boulders located in the fanhead (T2u) and decreasing clast size away from the fan apex with small boulders to cobbles located throughout the midfan (T2i) region and base (T2d) of the Biskra fan. Desert pavement is common to this surface, mainly between boulders as tightly compacted pebbles. Abundant varnish on cobbles and boulders on the fan surface, the presence of numerous fault scarps, and erosion by small gullies indicate the fan is no longer depositionally active. Current quarry excavations into the T2d fan segment reveal a thick sequence of alluvial sands and gravels ~80 m deep. Several well-developed paleosols indicate that the quarry probably exposes several buried alluvial fan complexes.

The upper portion of this fan is labeled as T2u in Plate I. Minor faulting disturbs the surface at the northeastern edge, where the modern wash has eroded away the southwestern edge of this surface. Some drill pads and roads cut portions of this fan, but otherwise the T2 surface is intact (Behr et al., in press). Large m-size boulders are found in the northern-most extent and exhibit a moderate degree of desert varnish (Behr et al., in press).

Located between the Mission Creek splays, T2i is the intermediate section of the prominent Biskra fan (Plate I). Similar to T2u, a series of fault scarps cut the northeastern extent of the surface, although minor faulting also occurs at the

southwestern portion as well. A series of swales exist and can be distinguished with some difficulty from the small-scale faults present on the surface (Behr et al., in press). Behr et al. (in press) describe a prominent stream incision that cuts this surface and aligns with a similar feature matching across the northern Mission Creek fault onto the SW splay of the MCS-SAF. This apparent correlation suggests little if any strike-slip offset has occurred across the NE splay.

The largest portion of the fan, the T2d section has largely been removed by quarrying. Mapping prior to quarrying showed that cobbles and small boulders embedded in the surface contained a notable amount of desert varnish, with desert pavement common throughout this surface. Swales on this surface match the overall trend of those found on T2i and appear to be unmodified since fan deposition due to boulders in the channels exhibiting the same amount of desert pavement as those on the fan surface (Behr et al., in press).

The presence of large granitic boulders on T2 makes it an ideal setting to apply the ^{10}Be and ^{26}Al cosmogenic dating technique. Heavy varnish on the tops of these boulders indicates long-term stability, satisfying a requirement of cosmogenic dating that a clast must appear in situ. Behr et al. (in press) and van der Woerd et al. (2006) chose this technique to date the fan surface for this reason, yielding ages of 45-56 ka and 35 ± 2.5 ka respectively.

The development of the Biskra fan in an arid setting limits the preservation of physical material for chronological dating. Formation of calcic soil horizons in the subsurface of the T2 fan provides sampling material. This

allowed Fletcher et al. (in press) to sample calcium carbonate rinds formed on cobbles in the subsurface of T2d, measuring the $^{230}Th/^{238}U$ concentrations yielding an age of 45.1 ± 0.6 ka.

T3

The oldest dated terrace level at Biskra Palms is the T3 surface, dated at 66 ± 0.6 ka by Behr et al. (in press). This surface lies to the northwest of T2i, between the splays of the Mission Creek faults (Plate I). Only a small remnant of this surface is preserved, with no upstream and downstream recognizable components intact (van der Woerd et al., 2006) and is back-tilted by a scissors fault that bounds the northwestern edge of T2i (Behr et al., in press). Clasts here display a greater amount of desert varnish, in comparison to the T2 surface (Behr et al., in press). In addition the T3 boulders are more weathered, with spalled margins and local grussified granite boulders (Behr et al., in press). Similar to T2, boulder tops were sampled by Behr et al. (in press) for cosmogenic age dating.

T4

T4 refers to a low-relief upland surface developed atop the Palm Spring Formation. Deep canyons and gullies cut the T4 surface. Numerous faults and folds have also deformed the surface. Here ponded alluvium accumulates locally against the fault scarps forming small basins. The T4 surface consists of cobbles and boulders and locally resembles the alluvial surface of the T2 fan. Scarce patches of desert pavement occur on T4. Large (>1 m) boulders litter the surface, some being heavily weathered with significant amounts of desert

varnish. Two possible interpretations may explain the presence of the boulders 1) the T4 surface may have once been a remnant of a broad alluvial plain (Ocotillo Fm.) and only the boulders remain with some alluvium or 2) the boulders were derived from the underlying Palm Spring Formation, with the finer material eroded away leaving behind a lag of boulders. It can be noted however, that the boulders and gravel do not seem to be included as a distinct layer within the Palm Spring Formation, but merely as a veneer overlaying the deformed strata.

STRUCTURES

Mission Creek Strand-SAF

The Mission Creek Strand-SAF consists of two splays about 400 m apart that are traceable across the study area (Plate I). Both splays strike N45W; the NE splay has a near vertical dip whereas the SW splay dips steeply to the NE, suggesting that the two splays merge with depth (van der Woerd et al., 2006). The SW splay exhibits strike-slip offset of geomorphic surfaces such as truncated and beheaded streams and offset alluvial fans. A vegetation lineament characterizes this splay with various grasses and shrubs and a row of palm trees growing in the fault zone. The NE splay is expressed by a topographic lineament with local depressions and uplifts. No obvious geomorphic displacements mark the NE splay. The faults cut all units except the recent alluvial units (T0) and are therefore considered active structures.

The T2 surface shows considerable oblique-slip displacement across the SW splay, with little oblique slip on the NE splay (van der Woerd et al., 2006; Behr et al., in press). The planar surface of T2i indicates back tilting of 22° as measured by Behr et al. (in press), between the NE and SW splays. Slip can be estimated using the apex of the T2 fan and shows ~770 m of dextral slip on the SW splay with no appreciable dextral slip across the NE splay (Figure 4) (Behr et al., in press). A beheaded stream and incised gully remain aligned on Figure 4 with no dextral offset across the NE splay.

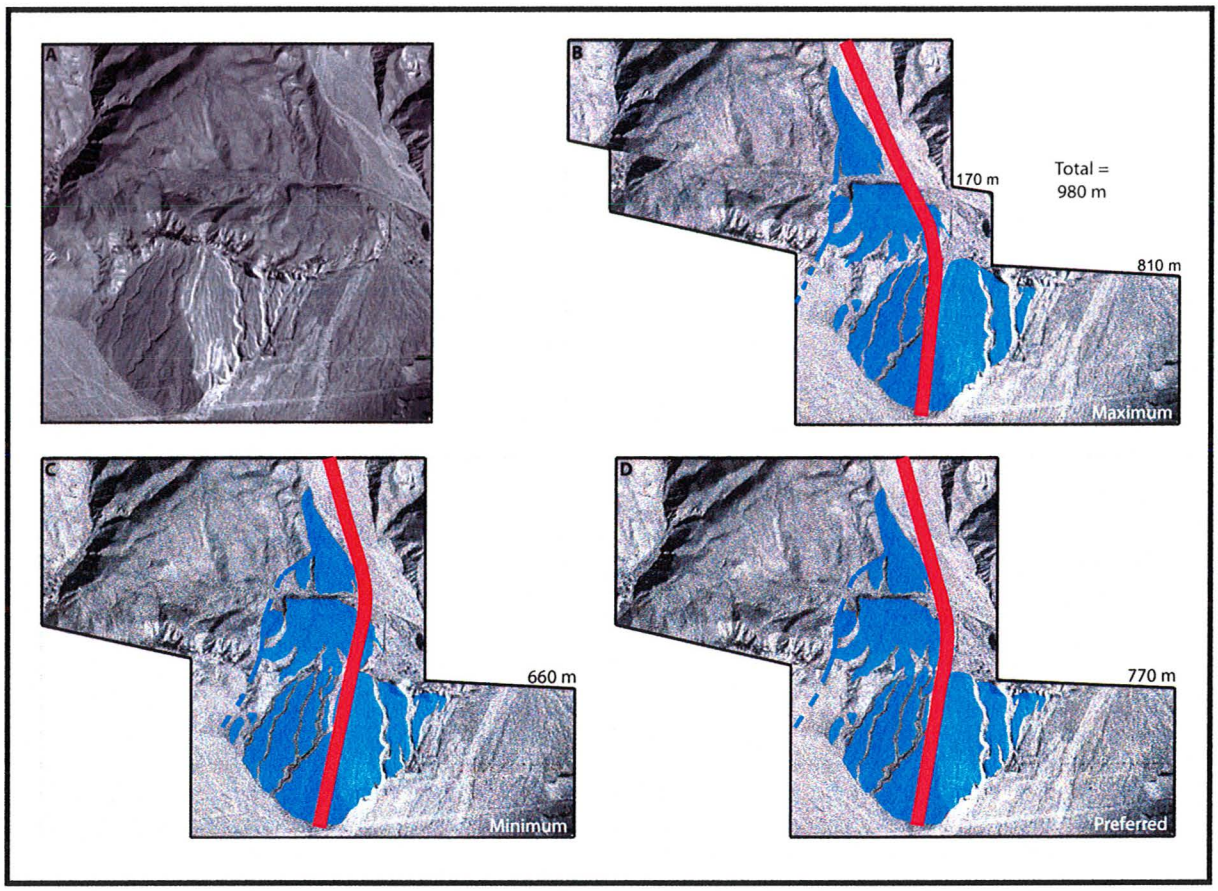

Figure 4. Reconstruction of Behr et al. (in press) of the T2 surface of the Biskra fan shown in blue. Their offsets take into account concealment of the lower fan surface, for which evidence was provided by this study. Using the apex of the fan, outlined in red, they ultimately choose a preferred offset of 770m as shown in scenario D.

Banning Strand-SAF

North of the study area the Banning fault forms a linear NW-striking right-lateral strike-slip fault that is oriented parallel to the MCS-SAF but bounds the western edge of the Indio Hills (Figure 3) (Keller et al., 1982; van der Woerd et al., 2006). At the base of the Indio Hills north of the Biskra fan, this splay changes from a dextral offset to a thrust, merging with the SW MCS-SAF at depth (Plate I). Geomorphic features outlined in Figure 5, such as escarpments,

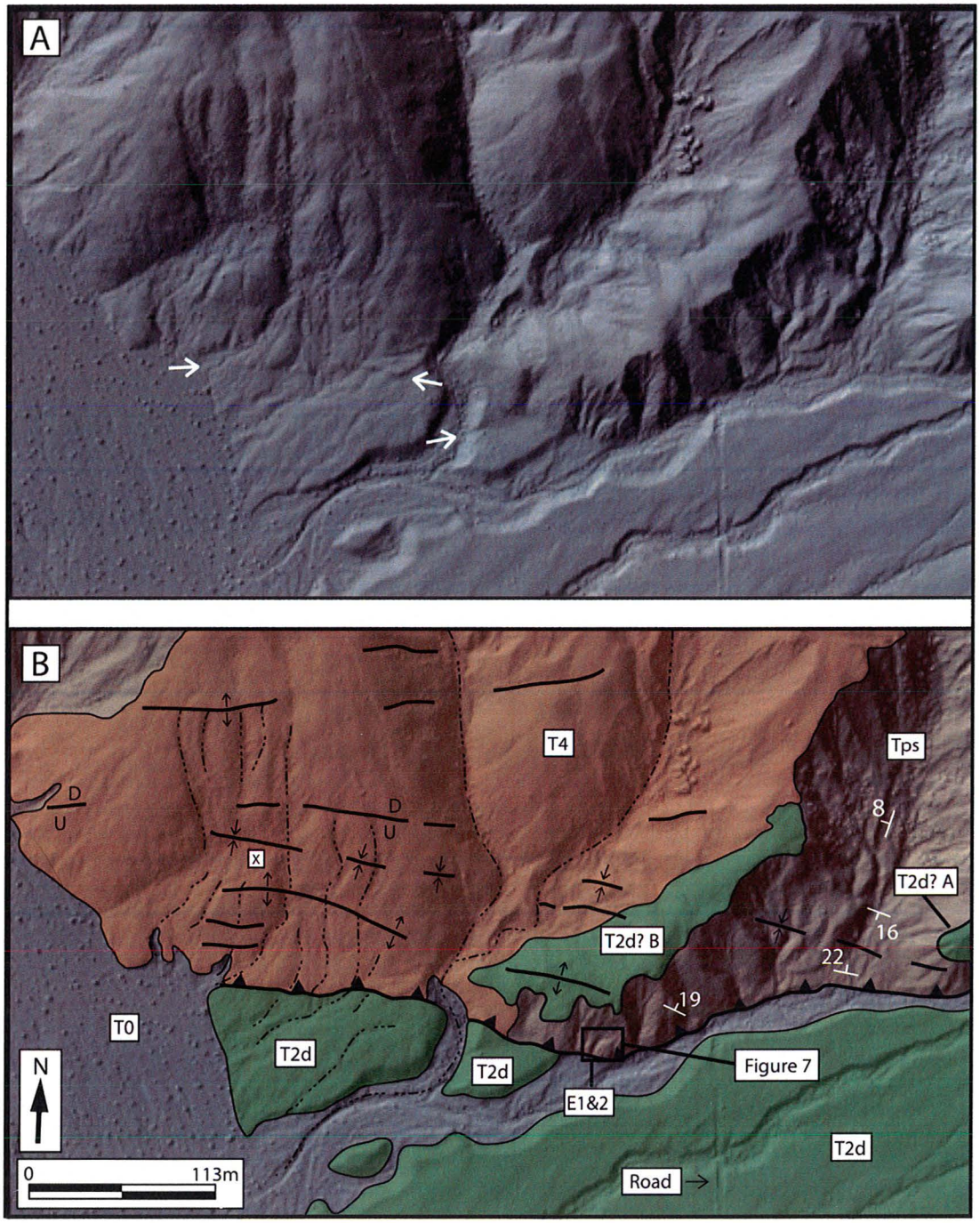

Figure 5. (A) LiDAR image of the northern end of the T2d fan at the base of the Indio Hills. (B) LiDAR image with geology superimposed. Bold black lines mark possible scarps; thin black lines locate gullies. T2d = green, T4 = orange, Tps = Palm Spring Fm., T2d?A and B = possible remnant surface in the hanging wall of the mapped thrust. Flat area at X that appears to be back-tilted T4 surface with deflected gullies. Subtle E-W scarp on LiDAR image between tips of arrows (A) that separates T4 from T2d (on B).

deflected and abandoned stream channels possibly outline the trace of the BS-SAF at the base of the hills north of T2d. The total amount of slip is unknown. Faulting cuts the Palm Spring Fm., placing older over younger units, truncating the NW edge of T2d an undetermined distance (This Study). A series of E to W trending folds in the Palm Spring Fm., lie sub-parallel to the trace of the BS-SAF (Plate III). The presence of highly unconsolidated slope colluvium mixed with Palm Spring Fm. discovered in the trench excavations places the latest faulting event as recent but with an unknown absolute age.

Secondary Faults

A series of N-S striking secondary faults occur at the Biskra site north of the T2d surface in the Indio Hills and are common on the T2u and T2i surfaces (Plate I). Escarpments are ~1 m high, face both to the east and west and are a few m in length. Locally, uphill-facing scarps and graben-like structures trap sand and fine gravel on T4 (Figure 6). Faulting clearly deforms the older terraces (T2 and T4). The largest fault-bounded basin occurs along the NE-MCF where motion across a secondary "scissors" type fault has back-tilted the T2i block, locally accumulating aeolian and alluvial/fluvial sands (Behr et al., in press). Alluvium found in these basins assumes a recent age of deformation of these units.

Folds

Strike and dips of bedding measured within the Palm Spring Formation reveal a series of folds trending ~ E-W with the dip of the limbs varying from 8° to 62° (Plate I). The interlimb angle of these series of upright anticlines and

synclines appear to be gentle to open in geometry. Numerous folds were mapped via the geomorphology in the Indio Hills NW of T2d, although symmetry can only be determined from exposed beds. Exposed units display gently folded limbs of ~20° to 40°. These bedrock folds appear to have deformed the T4 surface (Figure 5). Geomorphic features such as deflected stream channels and anomalous topography is correspondent to folding in the subsurface. Overall the folds are parallel to the thrust at the base of the hills and suggest a genetic linkage (Plate II).

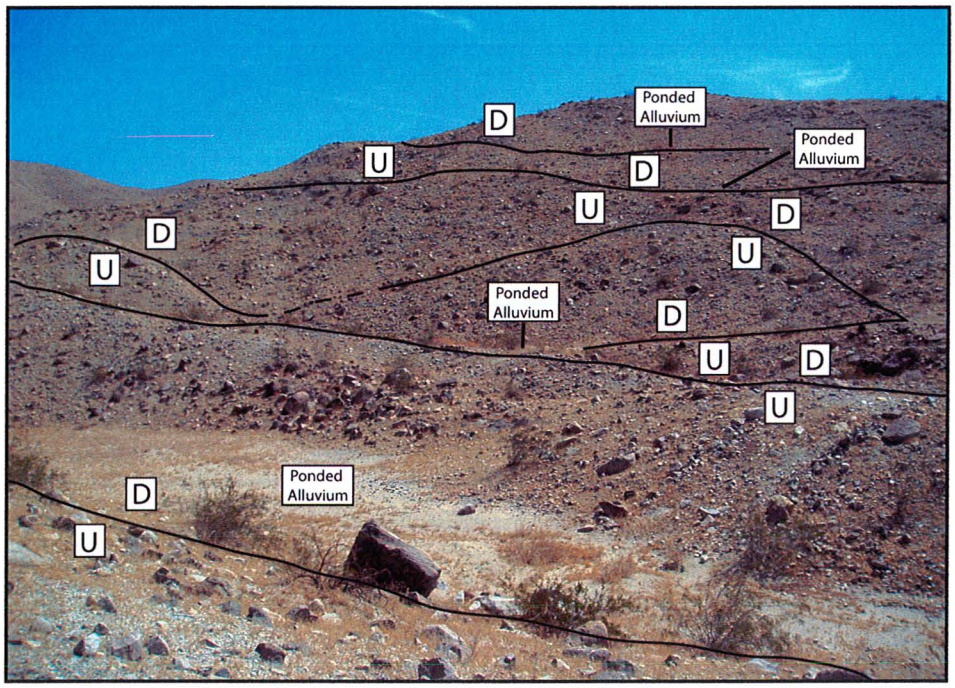

Figure 6. View looking north at fault scarps of secondary fault zone that cuts T4 to the north of excavations (Plate I). U and D (up and down) refer to sense of separation across fault scarps. Sand and fine gravel is ponded against uphill-facing scarps.

EXCAVATIONS

Overview

Several features are common to all excavation sites. Each excavation exposes a low-angle shear zone that separates a hanging wall comprised of Plio-Pleistocene Palm Spring Formation from a footwall comprised of latest Pleistocene T2d gravels and/or Holocene(?) colluvium and alluvium. The shear zone consists of poorly sorted fine- to medium-grained sands and gravels, derived from both hanging wall and footwall sediments. The Palm Spring Fm. in the hanging wall consists of alluvial/non-marine fluvial conglomerates, sandstones, siltstones and mudstones (Dibblee, 1954; Norris and Webb, 1976; Keller et al., 1982; Lutz et al., 2006; Behr et al., in press). Numerous faults dissect the Palm Spring Fm. with increased deformation near the shear zone. The T2d alluvium and Holocene(?) colluvium/alluvium in the footwall consist of loosely consolidated fine to coarse-grained sands and gravels with well-developed paleosols common for most surfaces. We abbreviate these said units in the following text and excavation logs as follows: Palm Spring Formation (PS), Sheared Palm Spring Formation (PSs), T2d Alluvium (T2), Shear Zone (SZ), Slope Colluvium (C1) and Faulted Colluvium (C2). See Table 2 for unit descriptions.

Table 2. Description of units observed in the excavations.

UNIT	DESCRIPTION
C2	Slope colluvium, poorly sorted with sand to boulder-sized clasts that consist of granite, gneiss and scarce Palm Spring Formation.
C1	Colluvium; similar to C2 but found beneath faults, up to 1.5 m thick. Locally contains 5 to 20-cm-thick lenses of thin bedded, well-sorted pebble gravel.
T2	Late Pleistocene alluvium with a well-developed reddish-orange (5yr 4/4) weathered soil. Alluvium primarily consists of cobble- and boulder-rich layers with secondary lenses of pebbly sand. Upper part of soil is 1.5 m thick, orange to reddish-orange with blocky pedz, weathered clasts, and translocated clays; lower part is an ~1-m-thick carbonate-rich accumulation zone (K horizon) with carbonate rinds on lower half of clasts.
SZ	Shear zone material; a mixture of lenses of Palm Spring Fm and C1 colluvium. Internal shear fabric is parallel to contact with overlying/ underlying units.
PSs	Palm Spring Fm, heavily sheared; structurally overlies SZ unit and consists of sheared local mudstone, rust-orange sandstone (10yr 6/6), and pebbly sandstone units. Shear fabric is parallel to faults.
PS	Slightly sheared Palm Spring Fm; Plio-Pleistocene, gray-green to grayish yellow sandstone with secondary mudstone and pebbly sandstone.

Excavation 1

This excavation consists of two cuts at a right angle to each other. E1a trends NE-SW and consists of a 50-m-long cut into a natural terrace riser of the T2d surface and bordering steep hillside (Figure 7, Plate I). A striking feature here is the reddish-orange soil of the T2d fan that extends beneath the base of the hillslope (Plate III).

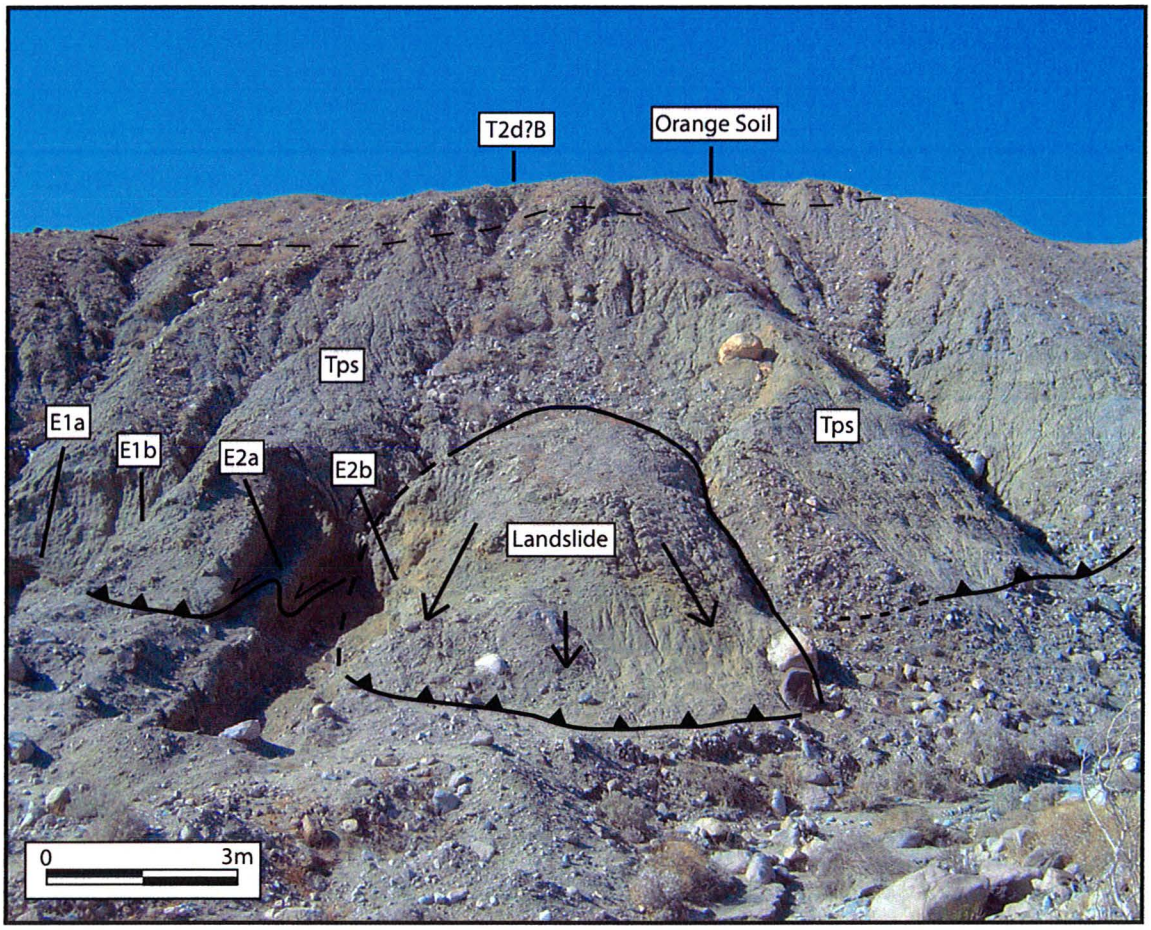

Figure 7. View to the north of excavations E1 and E2. The slide plane of a small landslide is exposed in E2b. An orange soil caps an alluvial strath terrace (T2d?B) cut into Palm Spring Fm. (Tps) in hanging wall of thrust.

This surface projects at an inclination of ~5-10° to the SW, parallel to depositional dip of the T2 alluvial fan. At the base of the reddish-orange paleosol horizon is a clast-supported coarse gravel unit. Here, accumulations of calcium carbonate rinds have formed on the undersides of gravel cobbles, which is indicative of arid climates (Blissenbach, 1954). Both the orange soil and calcic horizons maintain a uniform depth of ~0.5 m and ~ 1 m below the T2d surface, respectively, where they pass beneath the shear zone and the hillslope.

This excavation was cut parallel to a line of m-sized boulders that form a levee atop the T2d surface. This line of boulders extends beneath the hanging wall block relatively undeformed. The cut for this excavation is parallel to a riser of the original T2d surface and the modern gulley. The riser is exposed at the east end of E1a where gray colluvium (C1) overlies an ~20° south-dipping contact with the red-orange Bt soil of T2d. Both T2d and the colluvium underlie a shear zone (Plate III).

The connection of the E-W trending wall of E1a with the N-S trend of E1b at the eastern extent of E1a reveals a N63°E strike and 8-10° SE dip of the shear plane. The western extent of E1a exhibits a thicker shear sequence overriding the T2d fan where it consists of numerous splays and subsequently thins to the east separating sheared Palm Spring Formation from colluvium. The shear zone at the eastern end of E1a varies in orientation from 10-15° to the SSE, and changes from the dip of the shear zone at the west end of excavation 1 to ~15-20° E. I interpret this change to reflect where the shear zone overruns the terrace riser, an indication that the hanging wall is overriding topography.

The base of the shear zone consists of a clay gouge and a mixture of clasts above this zone, which consist of Palm Spring Fm. and igneous/metamorphic clasts of T2d and colluvium. Slickenlines in clay gouge at the base of the shear zone reveal a SSE trend. Above the shear zone, the Palms Spring Fm. may be heavily sheared although bedding is evident. Lenses of gravel in mainly a sand matrix define bedding within this unit. Overall, the apparent dip of bedding is sub-horizontal.

E1b. Excavation 1b trends NW-SE and consists of a 10-m-long excavation that intersects the NE end of E1a and extends into the modern wash at the foot of the T2d terrace riser (Plate III). The Palm Spring Fm. here appears massive, however it exhibits slight shearing of sand lenses and consists mainly of fine-medium grained sand. This unit overrides a thin clay gouge zone along a gentle 2° dip to the south.

The shear zone is ~0.2-0.3 m in thickness with a low SSE dip (see above). This unit consists of clay, fine to medium sands with rare gravels. No slickenlines were observed in the clay units.

At the base of the shear zone is a massive pebble-cobble colluvium in a fine-medium grained sand matrix. Local laminations of pebbly sand occur at the southern extent of this unit. Laminated pebbly sand resembles modern day wash deposits, akin to sands in a proximal stream channel south of this trench cut. Overall, colluvium is very indurated and resembles material found on the local slopes.

Excavation 2

E2a.

This excavation is located parallel to and a few meters NE of E1b (Figure 7). It consists of a cut into the base of the Indio Hills approximately 10 m long and the width of a trackhoe bucket with a bench on either side less than a meter wide (Plate IV). The Palm Spring Formation units here consist of mud and fine sandy layers. Prominent rust orange sands are distinctive as well as the shearing and folding of these units. Slickenlines in the gouge trend SE.

The base of the Palm Spring Fm. is bounded by a ~0.4 m thick shear zone to the NW thinning to the SE, becoming a depositional contact dipping ~15° to the SE. The shear zone consists mainly of massive mud and fine sands.

Structurally below the shear zone is a massive colluvial unit. Laminated fine sands are found within the upper portions of the colluvium, beneath the shear plane boundary and at the southern end of the exposure wall. At the northern terminus of the cut underlying the colluvial unit, a sliver of the T2 fan and the underlying calcic horizon paleosol is exposed. Progressively larger boulders are found at the south end of the excavation.

E2b. This exposure reveals highly sheared Palm Spring Fm. in the hanging wall of a shear plane that dips ~20° to the south. Here, thick bedding of the Palm Spring Fm. orange sands overlay muddy units, with multiple secondary shear planes and offsets within the unit. Overall, bedding of the Palm Spring Formation in the hanging wall terminates against a colluvial pile near the SE end of the trench cut. Units at this portion of the trench are characterized by slightly different lithologies. Light olive grey sands containing very-well rounded cobbles distinguish the PS Fm. sediments here. The northern end of E2b exposes a block of Palm Spring Formation with vertical bedding. The block overrides colluvium along a sub-horizontal sheared boundary. The block and the lower shear zone are buried by colluvium. This block of Palm Spring Formation, lower shear zone, and colluvium are cut by an upper sub-horizontal shear zone that can be followed for ~10 m to the south along the base of the upper wall (Plate IV).

In turn the upper shear zone is buried by colluvium at the base of the upper slope.

Bounding this unit is a thin shear zone, ~0.3 m in thickness that dips ~20° in the NW of the excavation, becoming a sub-horizontal depositional contact to the SE. This unit consists of a mixture of orange sands derived from the Palm Spring Fm. and coarse gravelly sand and mud. Within the muddy units, south-trending slickenlines are exposed.

A colluvial unit of cobbles and small to medium boulders in a medium-grained coarse sand matrix make up the footwall. Large cobbles and small boulders at the base of the hillslope are imbricated parallel to the slope. Orientations of these imbricated clasts are analogous to what is observed in E2a. Pockets of local laminated sands are found at the south end of the colluvium, ranging in size from small local pockets to larger deposits ~0.5 m in thickness.

Excavation 3

E3a. The lower segment of the T2d fan is a typical alluvial fan characterized by a gently dipping slope, presumed to be the original depositional dip. A small scarp occurs in the northeast corner of T2d, near the SW splay of the MCS (Plate I). E3a is a north-south trending exposure along the west-facing slope of this feature.

The hanging wall shows bedding of the Palm Spring Formation that dips ~15-20° to the north. Sheared layers of Palm Spring Fm. bedding typify this unit, including interlayered mud, medium-grained orange sands, and fine gravels (Plate V). Bedding in the hanging wall is cut by antithetic SE-dipping normal

faults that are consistent with top-to-the southeast sense of shear. Thinning beds and sheared Palm Spring Formation sediments characterize the shear direction (Figure 8). The southeastern extent of this feature has been deformed upwards and may indicate reworking.

A wide shear zone separates colluvium in the footwall from Palm Spring Formation in the hanging wall. Characterizing this zone is a mixture of mud and sand units derived from the hanging wall and coarse sand and cobbles from the footwall. At least two shear planes are identifiable. They cut this unit and terminate into a colluvial pile at the southeastern end of this excavation. Underlying the shear zone is a colluvial unit, exhibiting a non-bedded thick sequence of cobbles and small boulders in an oxidized reddish matrix. This unit overrides the T2d fan surface, which is characterized by the reddish paleosol seen prominently in E1a (Plate III). Pockets of laminated sands, denoted as Qal? on the excavation log of E3a (Plate V), are located between the cobbles and small boulders of what may be have been the fan surface. The southern terminus of this cut reveals a thin block of slope colluvium. The continuation of this unit was removed to produce excavation 3b, which resides perpendicular to this excavation wall. Imbrication of clasts within the colluvium and the chaotic deposition or tractor tread-like orientation of the cobbles, possibly indicate multiple episodes of movement within these units.

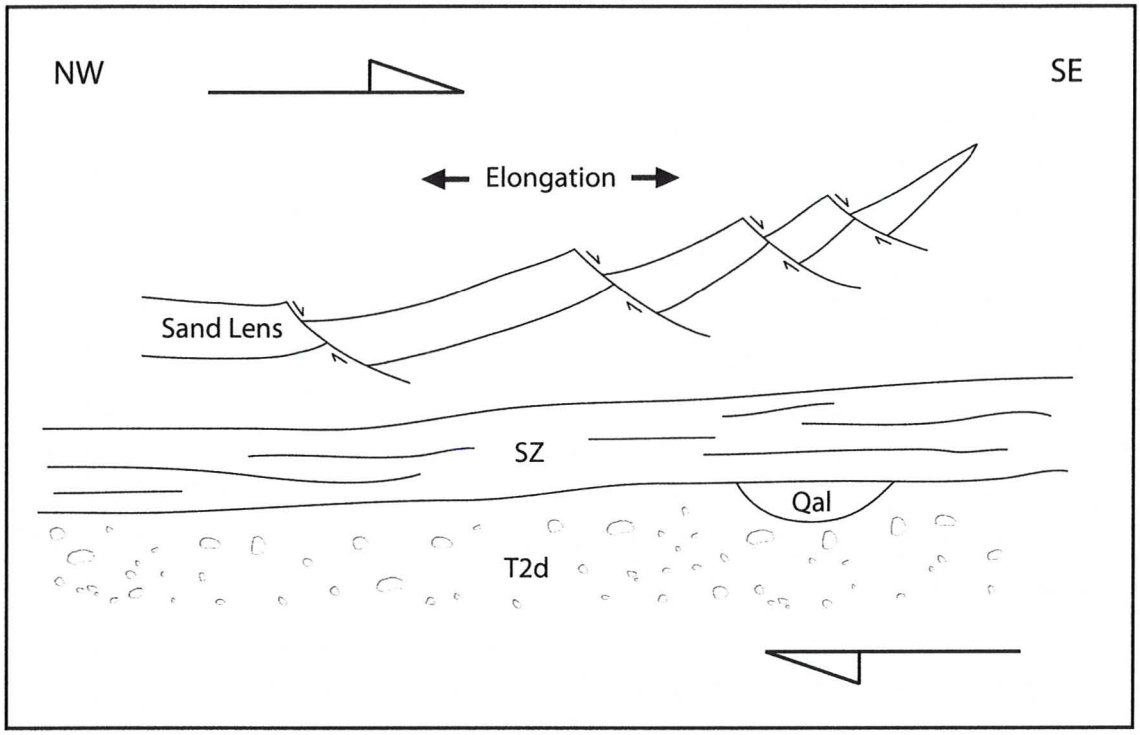

Figure 8. Schematic drawing of the sheared sand lens cut by antithetic faults exposed in excavation 3a (Plate V). Offset of this feature indicates movement to the southeast in the hanging wall overriding a shear zone (SZ) mixture of Palm Spring Fm. and colluvium. Note the development of modern alluvium on the T2 fan surface (Qal).

E3b. This trench trends NE-SW and is perpendicular to excavation 3a at the base of a small escarpment on the T2d surface (Plate I). The E3b cut completes a 3-D cut through the fault block. The Palm Spring Formation in the hanging wall consists of alternating silt, sand, and gravel layers that are parallel to a sub-horizontal shear zone. Many of the sedimentary layers appear to be bounded by sub-horizontal faults presumed to be the normal-style faults observed in E3a. Whereas E3a is cut parallel to their dip direction, E3b is cut parallel to their strike. An orange sandy unit common in other excavations is present as multiple strands interfingered within a grey sand unit. To the southwest within the

excavation, sediments in the exposure become greatly mixed with medium-grained sands becoming warped containing an occasional cobble. Strands of sheared carbonate lenses are interlayered within the sand units. The termination of this unit buttresses against the colluvium discovered at the southeastern extent of E3a.

The trace of the shear zone unit becomes faint, nearly indistinguishable from the Palm Spring Formation as it extends to the southwest, becoming more defined to the northeast. At this portion of the excavation a distinct contact between shearing and colluvium is observed.

Large cobbles in a coarse gravel-sand matrix are common in the colluvium, containing fewer boulders than seen in other colluvial piles exposed, with the exception of a very large schist boulder. This anomalous boulder is preserved in the colluvium with its nearly meter long axis situated vertically. Assuming movement due to faulting, this boulder signifies movement to the southeast, which is congruent with findings in E3a. Colluvial grain size decreases towards the intersection with the southeastern segment of E3a, becoming a mixture of coarse sand and gravels with sparse cobbles and boulders.

The unit beneath the colluvium consists of large stacked cobbles in a sand matrix, which is likely a continuation of the unit defined as T2 in E3a. It is unclear whether this unit may really be the T2 fan surface.

DISCUSSION

Depositional vs. Structural Edge of T2d

Previous slip estimates across the San Andreas fault at Indio hinged upon reconstructions that consider the NW margin of T2d, T2i and T2u to represent the depositional edge of the late Pleistocene T2 alluvial fan (Keller et al., 1982; van der Woerd et al., 2006). However, mapping and trench excavations by this study, and also Behr et al. (in press), show unequivocally that this feature has been overridden by a low-angle shear zone (Figure 2b). This observation requires that the true depositional edge occur some unknown distance to the north. Either it must reside in the footwall of the thrust some unknown distance to the northwest, or it must reside in the hanging wall if the thrust cut through a piece of the T2d fan as it moved. The previously considered margin of T2d therefore does not accurately record the strike-slip offset that post-dates cessation of deposition on the T2 fan. Using this feature as a piercing line will instead provide a minimum slip estimate for the San Andreas fault over the past ~50 ka. Plate I shows possible strath terraces (T2d?A & B) cut into the Palm Spring Fm. that resemble the T2d fan gravels (Figure 9). This supports the possible interpretation that the depositional edge of the T2d fan occurs in the hanging wall of the thrust, if the strath gravels indeed correlate with the T2d surface in the footwall.

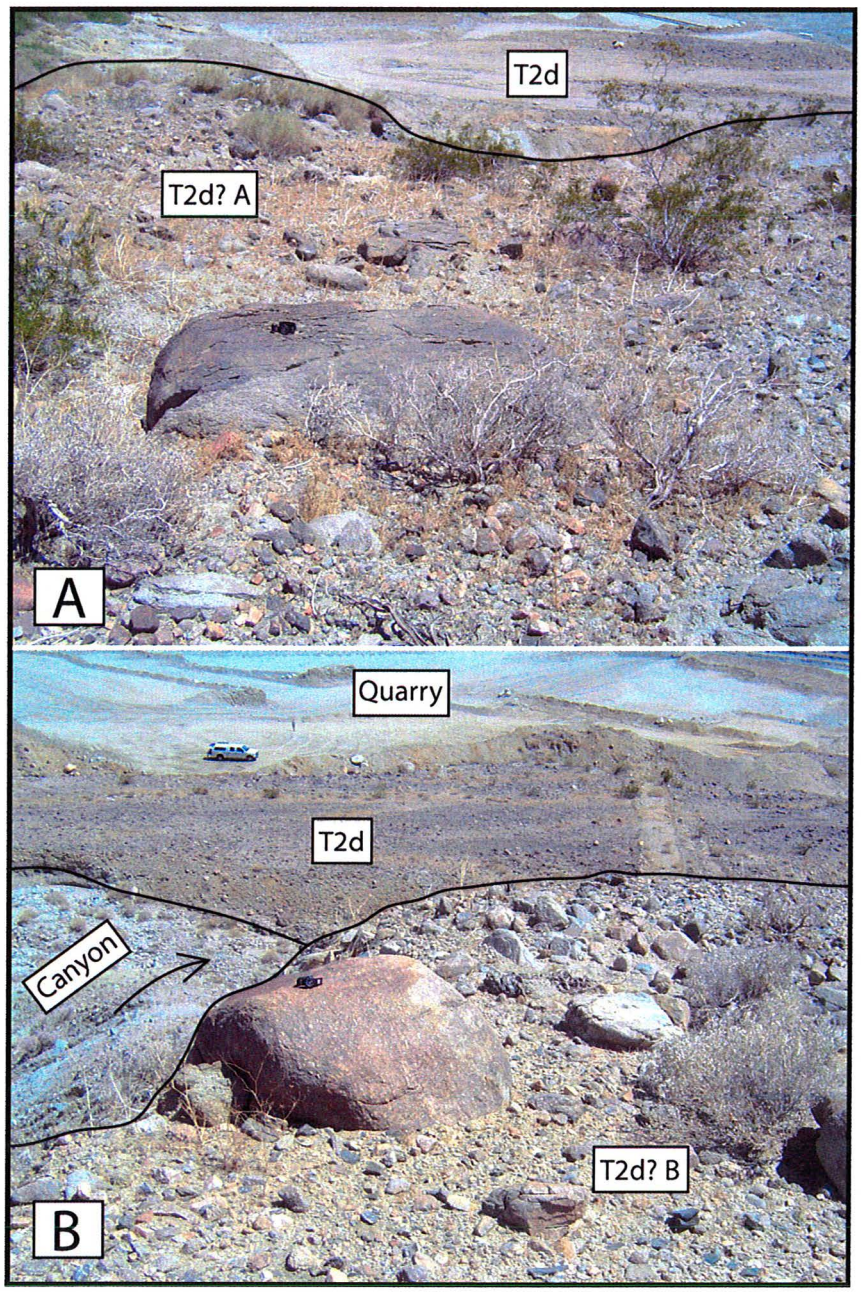

Figure 9. Foreground view looking south across erosional remnants of T2d? surfaces in hanging wall of thrust. Background view is T2d in footwall. A) eastern remnant. B) western remnant. Desert varnish development on boulders (wristwatch for scale) in A and B is similar to that observed on T2d in footwall. T2d? appears more deflated than T2d probably due to faulting and enhanced erosion in hanging wall block.

Intersection of the Banning and Mission Creek fault strands

It has long been recognized that the Banning and Mission Creek strands of the Coachella Valley segment, San Andreas fault merge at Biskra Palms Oasis. However, several interpretations have been proposed for how this fault interaction occurs. Small-scale maps (e.g., Dibblee, 1954; Jennings, 1994) show linear traces of the Banning and Mission Creek faults that merge at Biskra Palms but do not show sufficient detail to distinguish where this occurs relative to the T2d fan. Keller et al. (1982) shows the Banning strand concealed by the T2d fan as it merges with the Mission Creek strand. This implies that the Banning strand has been inactive for at least the last ~50 ka as it merges with the Mission Creek strand. Clark (1984) and van der Woerd et al. (2006) show the Banning fault as a thrust fault that is concealed by the T2d fan, also implying that the Banning fault is inactive. The discovery for this study of a low-angle structure that overrides the north edge of T2d (Figure 2B) requires a revision of previous interpretations for faulting here. One possibility is that the low-angle structure revealed by my trench excavations (E1-E3) represents the slip plane at the base of a large landslide. Alternatively, this structure may represent the surface expression of the Banning fault. The following discussion explores the evidence in support or against the landslide and Banning thrust fault hypotheses.

Landslide Hypothesis

A central part of this thesis is the focus on the low-angle structures discovered in the trench exposures. It can be argued that the sub-horizontal slip plane represents the base of a landslide concealing the lower Biskra fan surface.

Hummocky topography on the Indio Hills north of T2d indicates a NW to S to SW downslope direction. A series of small secondary faults containing ponded alluvium in the Indio Hills, trend parallel to a SW downslope movement, supporting a landslide hypothesis (Figure 6). The sub-horizontal slip plane truncating the T2d surface may indicate that a slide concealed the fan surface.

However, several features in the excavations render a SW movement of the hills north of T2d as invalid. Slickenlines in clay gouge at the base of the shear zone in E1a show a SE trend (Plate I). A sheared sand lens in E3 exhibits a series of antithetic normal faults with extension to the SE (Figure 8, Plate V). A small landslide exposed in E2b, shows slickenlines at the base of the shear zone dipping 18° to the SE and striking of S20°W (Figure 7, Plate IV). A possible headscarp in region '2' on Figure 10 requires about 300 m of dextral slip on the NE Mission Creek fault, over twice what van der Woerd et al. (2006) estimated. Behr et al. (in press) interpret no strike-slip across the NE-Mission Creek fault, further discrediting this as a headscarp (Figure 4). If region '2' is a headscarp for a landslide exposed in E1-E3, this requires >2 times the slip supported by geologic arguments. Another possibility is that the headscarp for the landslide is the splays of the MCF. This would be a coincidence that headscarps occur where active splays of the MCF are projected. A simple interpretation is that these are not headscarps, but just the active splays of the MCF.

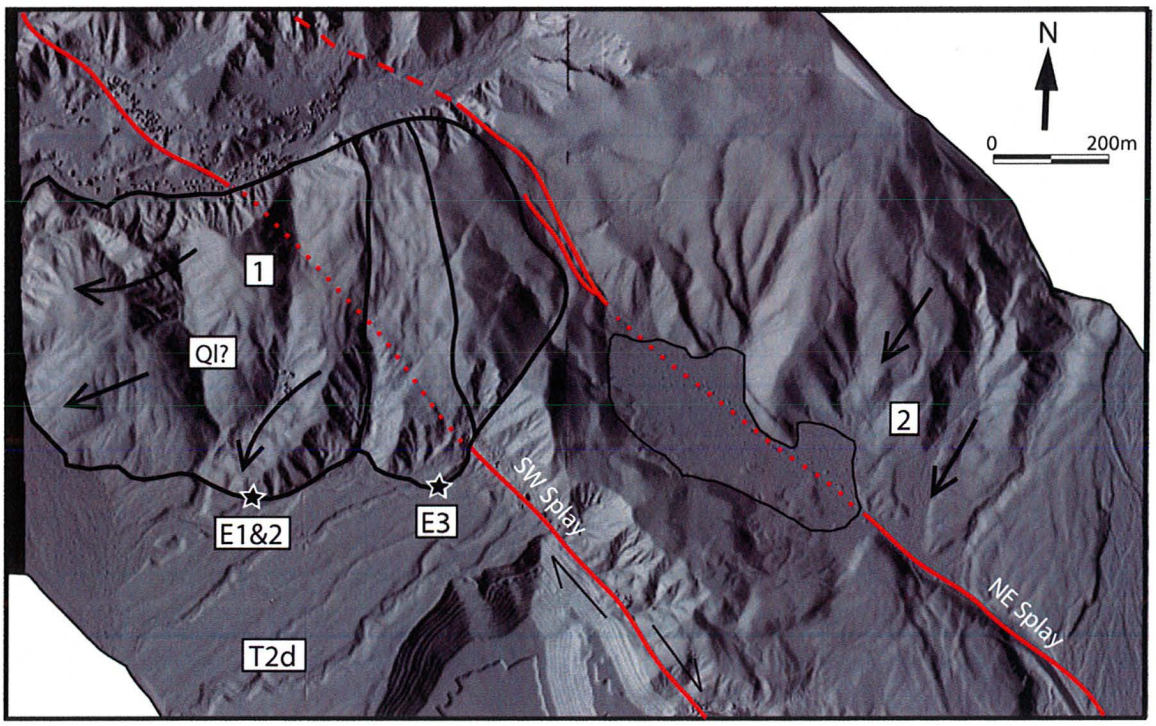

Figure 10. Landslide model that interprets the structure in E1, E2, and E3 as the toe of a landslide, not a thrust fault. (1) Landslide with headscarp at NE splay of MCS-SAF. (2) Head of larger landslide displaced in a right-lateral sense across NE splay MCS-SAF. This model requires ~300 m of dextral slip that is not supported by reconstructions of the T2 fan surface (van der Woerd et al., 2006; Behr et al., in press).

Thrust Fault Hypothesis

In order to better quantify the structure of the Indio Hills northwest of T2d, thorough mapping of the Palm Spring Formation was completed. Strike and dip measurements on Plate I suggest a series of folds of which the fold axes vary in trend ~E-W and are shown in cross-section in Plate II. This alignment of folding is inconsistent with deformation due to slumping, as this would produce a broad series of verging folds that trend NW-SE, perpendicular to the presumed direction of gravity sliding. The Banning strand is mapped bounding the western

edge of the Indio Hills, and has been inferred as being buried by the T2d fan to SE (Clark, 1984; van der Wored et al., 2006). Thus, folding in the Palm Spring units may be deformation due to the BS-SAF exhibiting a thrust component as it aligns with the southwestern Mission Creek splay.

Topography north of T2d where it meets with the Indio Hills contains scarp-like features outlined on Lidar imagery in Figure 5. These geomorphic features strike northwest and face south-southwest. Small gully drainages at the base of the hills here appear to be diverted and back-tilted. Also, undulating topography in the hills north of these escarpments coincide with strike and dip measurements, indicating a series of E-W folds in the subsurface. Although, no trenching was conducted at this site it is plausible these escarpments and offsets may be fault-related and may outline the trace of the BS-SAF. Findings in the excavations are consistent with this hypothesis, as they may have exposed the tip of a fault in the subsurface.

Remnants of the T2d surface may exist in the hills north of T2d. In Plate I, these surfaces are labeled as T2d(?) and are found in the hanging wall of the proposed thrust fault. Although, the surface of the Indio Hills has been characterized as an upland surface (T4) or the Ocotillo Formation, the possible remnants of T2 are distinct. A degraded pebble-cobble desert pavement is one of the most distinctive aspects of this surface and is more developed than the surrounding surfaces, perhaps because it is younger (Figure 9). Cliff faces north of T2d exposes a reddish paleosol in the subsurface of these patches (Figure 7). This may be the same age paleosol of the T2d fan and suggests truncation and

uplift on what was once the northwestern portion of the original fan surface. Remnant pieces of the fan in the hanging wall of this structure are consistent with thrust motion. A landslide event may have transported these surfaces downslope, however the lack of deformation on these surfaces more likely suggests uplift.

The prominent scarps in the northeastern portion of the T2d fan provide essential evidence for a thrust fault. Excavation 3 was placed along the most notable scarp in this locale and trends northeast to southwest. Bedding in the Indio Hills to the north of this feature strikes northeast and dips 16°- 40° to the northwest (Figure 11). These orientations are parallel to the scarp on the fan surface and suggest that a thrust front was exposed in excavation 3. A series of smaller scarps are located at the northeastern edge of the T2d at the base of an exposure of Palm Spring Formation as well (Figure 11). Here, bedding in the Palm Spring Formation strikes northwest and dips 27° to the northeast. This is consistent with the escarpments that strike to the northwest. An overall movement to the S-SE of the hills north of T2d is supported by the mentioned evidence and is highlighted in Figure 12, showing a thrust transport direction nearly perpendicular to a gravity slide. If indeed the BS-SAF exhibits a thrust component, it must steepen with depth to the north. This implies that the BS and MCF form a compressional stepover in the SAF system here, with oblique convergence being accommodated at the surface via thrust motion on the BS-SAF.

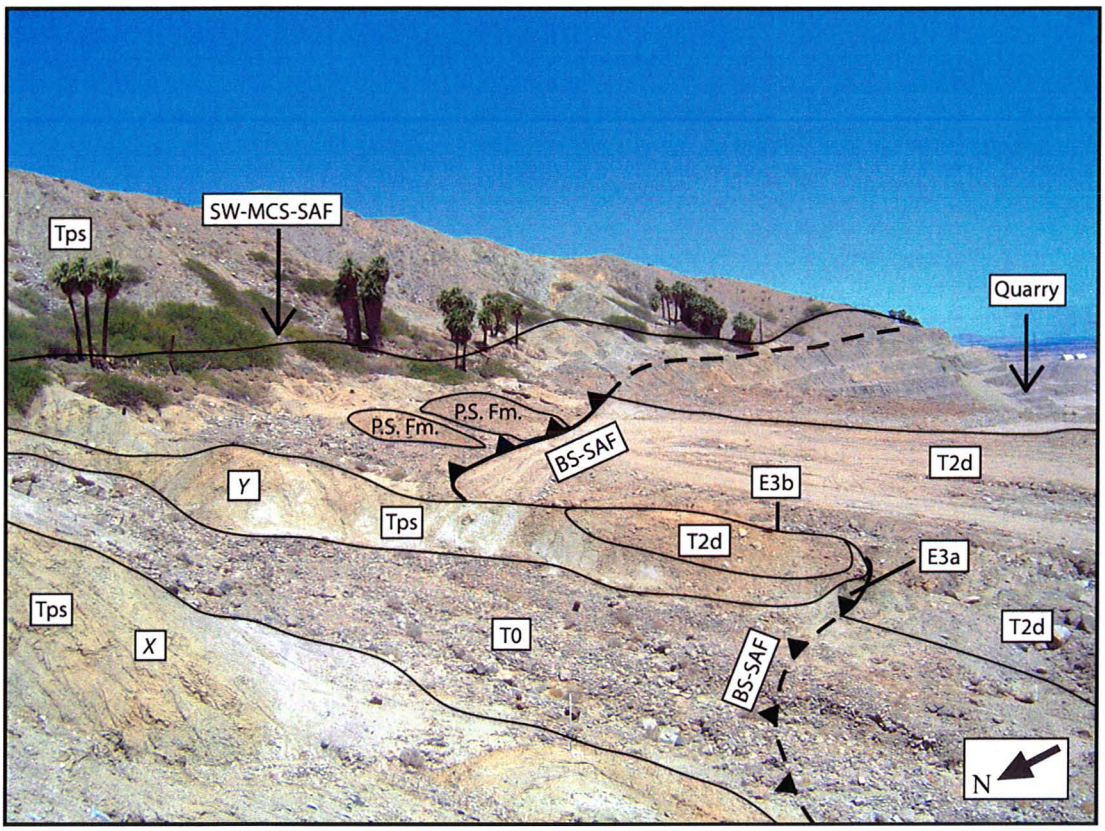

Figure 11. View to the southeast where the BS-SAF merges with the SW splay of MCS-SAF. Palm Spring Formation (Tps) exposed as remnants in hanging wall of BS-SAF, locally capped by T2d (at E3a). Bedding within the Palm Spring Formation dips 40°NW at *X* and dips 27°NE at *Y*.

Implications for Slip Rate

Measuring long-term slip rates across the southern San Andreas fault has proven difficult due to the lack offset geomorphic features. The distinct alluvial fan at Biskra Palms perhaps provides the most noticeable offset feature for this portion of the fault. The establishment of an accurate slip rate at Biskra Palms is crucial, as it known that very little slip has occurred on this segment of the fault since ~1680 (Sieh and Williams, 1990; Fumal et al., 2002). This accumulated strain poses increasing seismic hazard to the Coachella Valley as

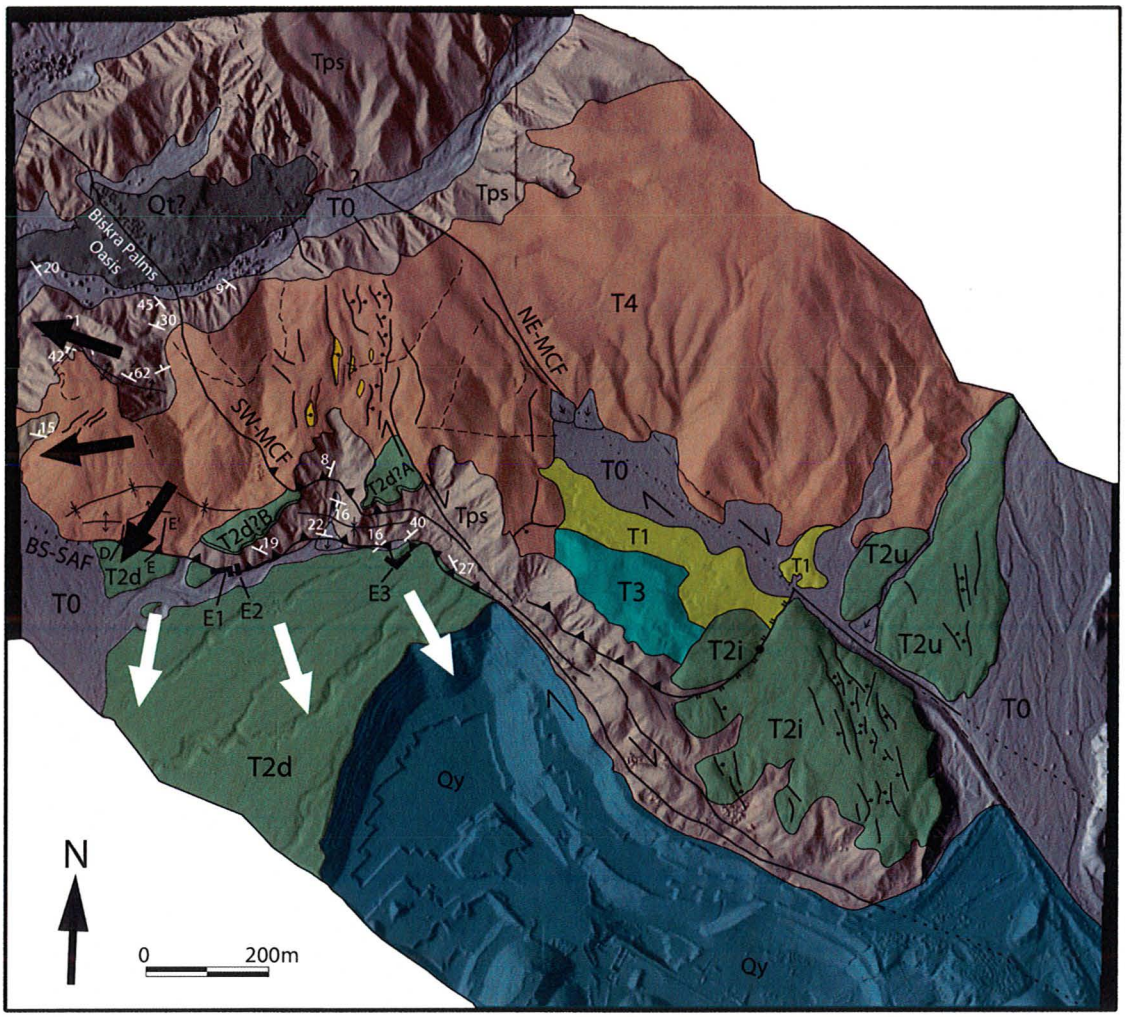

Figure 12. Geologic map (Plate I) with arrows showing movement of the hanging wall if landslide (black arrows) or thrust (white arrows). Excavations and mapping support a movement to the S-SE, which parallel the mapped trend of the BS-SAF as it merges with the SW-MCF.

well as major metropolitan areas in southern California. As excavations in this study reveal, the northwestern periphery of the T2d surface has been modified. This information renders the piercing lines used by Keller et al. (1982) and van der Woerd et al. (2006) (Figure 13) as invalid, changing the perceived offset of the fan. This study does not set out to calculate a new slip rate on the southern San Andreas fault. Findings discussed in this thesis, however, were contributed

to the Behr et al. (in press) study, leading to a reevaluation of the slip rate at this site. Since the true stratigraphic edge of the fan was not found in this study, Behr et al. (in press) used a probable apex of the fan to estimate the true fan edge (Figure 4). They use a preferred offset of 770 m on the southwestern Mission Creek splay, assuming little to no movement on the northeastern splay due to a prominent through-going stream channel on T2u that matches up with a channel on T2i. They interpret the break in topography of T2u from T2i as a structural break separating the two warped surfaces, rather than a faulted offset. With a newly constrained age of the fan surface of 45 to 56 ka, a slip rate for the Mission Creek fault was calculated at ~12 and 22 mm/yr with a preferred rate of ~14-17 mm/yr (Behr et al., in press).

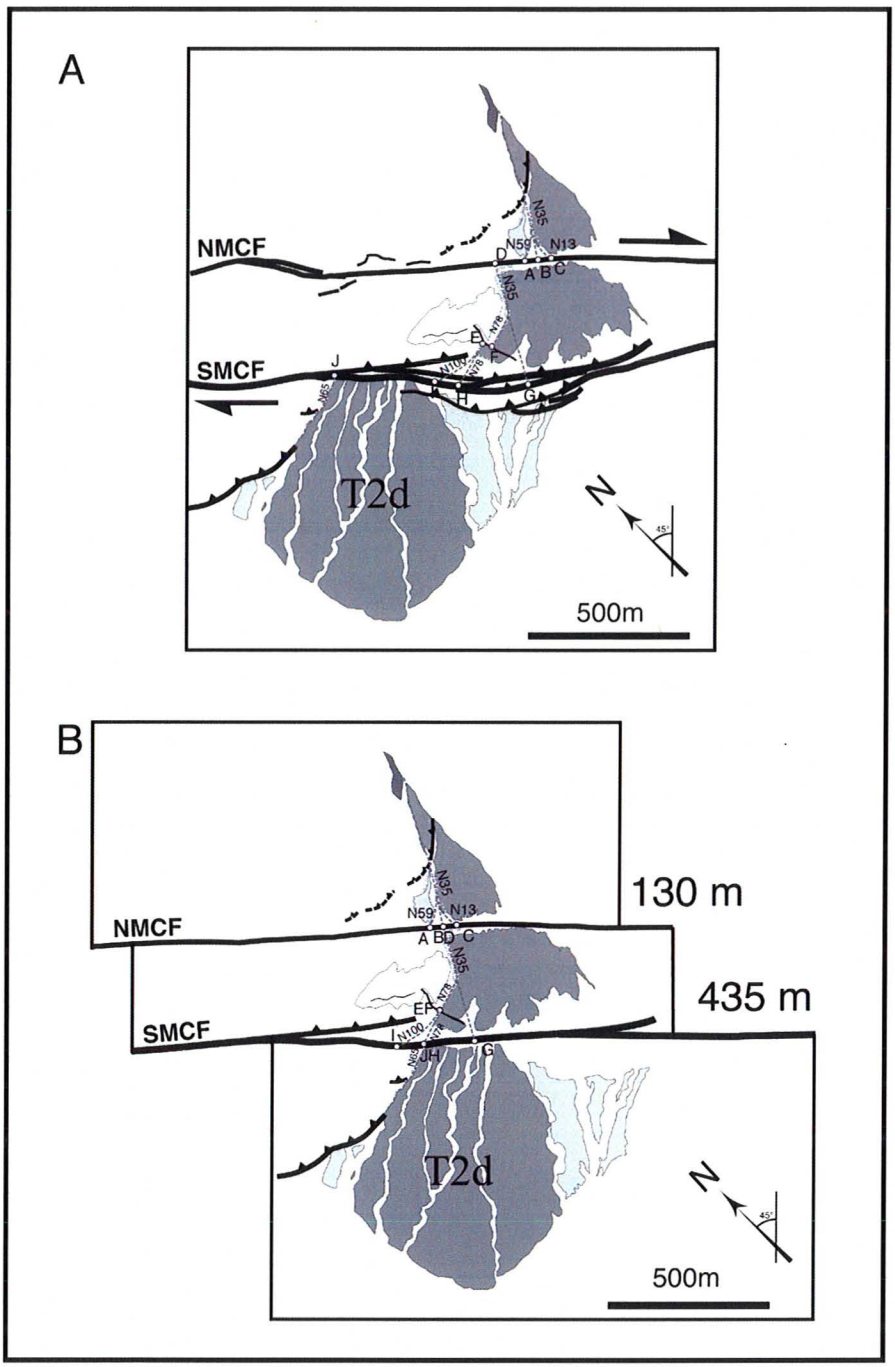

Figure 13. Reconstructed T2 fan surface from van der Woerd et al. (2006) showing 130 m and 435 m of dextral slip on the N and S splay of the MCS-SAF, respectively. This study shows that the northern margin of T2d is structurally controlled and is not a reliable piercing line for estimating slip.

CONCLUSIONS

Paleoseismic studies along the southern San Andreas fault provide crucial information relating to seismic events. Fumal et al. (2002) deduced that this portion of the fault is near failure and thus it is crucial to constrain an accurate slip rate here. The prominent offset of the Biskra Fan is a model for which to determine a slip rate, being that it seems a rather easy task to reconstruct the fan and undertake offset measurements. As has been discussed, the geology of the Biskra Palms site has proven surprisingly difficult to resolve and the apparent offset of the fan margin does not represent the true lithologic boundary. A detailed geologic map provided by this study reveals complexities in the hills to the north of the T2d fan surface. Excavations at the base of these hills on the northern extent of T2d show a low-angle structure overriding the northern periphery of the Biskra fan.

Based on bedrock geometries in the hanging wall of this feature and observations gathered from excavations, we conclude that the Biskra fan is being overridden by thrusting on the BS-SAF with a transport direction to the SE. It is also concluded that this thrust front merges with the MCS-SAF southwestern Mission Creek splay. These inferences change the location of piercing lines for the fan and thus change the overall estimated slip rates of Keller et al. (1982) and van Der Woerd et al. (2006). Although, it is concluded that the northern edge of T2d has been modified, the location of the true stratigraphic edge lies some unknown distance to the north-northwest.

The likelihood that the feature highlighted in Figure 10 is a landslide block is discounted for the following reasons. The subsurface of this block has been determined to be more structurally complex according to strike and dip measurements. Overall, trending E-W folds mapped in this block are oriented in a way that is inconsistent with gravity sliding; i.e. one would expect NW-SE trending folds oriented perpendicular to SW directed gravity sliding. In addition, sense of shear indicators in the shear zone and in the hanging wall indicate SE-directed transport, consistent with expected slip on the BS-SAF.

REFERENCES

Becker, T.W., Hardebeck, J.L., and Anderson, G., 2005, Constraints on fault slip rates of the southern California plate boundary from GPS velocity and stress inversions: Geophysical Journal International, v. 160, no. 2, p. 634-650.

Behr, W.M., Rood, D.H., Fletcher, K.E., Guzman, N., Finkel, R., Hanks, T.C., Hudnut, K.W., Kendrick, K.J., Platt, J.P., Sharp, W.D., Weldon, R.J., and Yule, J.D., in press, Uncertainties in slip rate estimates for the Mission Creek strand of the southern San Andreas fault at Biskra Palms Oasis, southern California, Geological Society of America Bulletin, *in press*.

Bennett, R.A., Rodi, W., and Reilinger, R.E., 1996, Global positioning system constraints on fault slip rates in southern California and northern Baja, Mexico: Journal of Geophysical Research-Solid Earth, v. 101, no. B10, p. 21943-21960.

Blake Jr., M.C., Campbell, R.H., Dibblee, T.W., Jr., Howell, D.G., Nilsen, T.H., Normark, W.R., Vedder, J.C., and Silver, E.A., 1978, Neogene Basin Formation in Relation to Plate-Tectonic Evolution of San Andreas Fault System, California, American Association of Petroleum Geologists Bulletin, v. 62, no. 3, p. 344-372

Blissenbach, E., 1954, Geology of Alluvial Fans in Semiarid Regions, Geological Society of America Bulletin, v.65, p. 175-190.

Brothers, D.S., Driscoll, N.W., Kent, G.M., Harding, A.J., Babcock, J.M., and Baskin, R.L., 2009, Tectonic evolution of the Salton Sea inferred from seismic reflection data, Nature Geoscience 2, p. 581-584, doi:10.1038/ngeo590.

Burciaga, A., Yule, D., Howland, C., Behr, W., Dawson, S., and Lee, V., 2004, A 2000-year-long record of large earthquakes on the San Bernardino strand of the San Andreas Fault, San Gorgonio Pass, Southern California, Seismological Research Letters, v. 75, no. 2, p. 293.

Clark, M.M., 1984, Map showing recently active breaks along the San Andreas fault and associated faults between Salton Sea and White-water River-Mission Creek, California, U.S. Geological Survey Miscellaneous Field Investigation Map, I-1483, scale 1:24,000.

Dair, L., and Cooke, M.L., 2009, San Andreas Fault geometry through the San Gorgonio Pass, California, Geological Society of America, Geology, v. 37, no. 2, p. 119-122.

Dibblee, T.W., Jr., 1954, Geology of the Imperial Valley region, California: California Division of Mines and Geology Bulletin 170, p. 21-28.

Dokka, R.K., and Travis, C.J., 1990, Role of the Eastern California Shear Zone in accommodating Pacific-North American Plate motion, Geophysical Research Letters, v. 17, p. 1323-1326.

Dolan, J.F., Bowman, D.D., and Sammis, C.G., 2007, Long-range and long-term fault interactions in Southern California, Geological Society of America, v.35, p. 855-858, doi: 10.1130/G23789A.1.

Dorsey, B., 2002, Late Pleistocene slip-rate on the Coachella Valley segment of the San Andreas fault and implications for regional slip partitioning: Cordilleran Section GSA 99th Annual Meeting, Puerto Vallarta, Jalisco, Mexico, 1-3 April.

Fay, N.P., and Humphreys, E.D., 2005, Fault slip rates, effects of sediments and the strength of the lower crust in the Salton Trough region, Southern California: Journal of Geophysical Research, v. 110, p. B09401, doi: 10.1029/2004JB003548.

Fialko, Y., 2006, Interseismic strain accumulation and the earthquake potential on the southern San Andreas fault system: Nature, v. 441, no. 7096, p. 968-971.

Fletcher, K.E.K., Sharp, W.D., Kendrick, K.J., Behr, W.M., Hudnut, K.W., and Hanks, T.C., in press, Th230/U dating of a late Pleistocene alluvial fan along the southern San Andreas fault, Geological Society of America Bulletin, *in press*.

Fumal, T.E., Rymer, M.J., and Seitz, G. G., 2002, Timing of large earthquakes since AD on the Mission Creek strand of the San Andreas fault zone at Thousand Palms Oasis, near Palm Springs, California: Bulletin of the Seismological Society of America, v. 92, no. 7, p. 2841-2860.

Harden, J.W., and Matti, J.C., 1989, Holocene and Late Pleistocene Slip Rates on the San Andreas Fault in Yucaipa, California, Using Displaced Alluvial-Fan Deposits and Soil Chronology: Geological Society of America Bulletin, v. 101, no. 9, p. 1107-1117.

Jennings, C.W., 1994, Fault activity map of California and adjacent areas with location and ages of recent volcanic eruptions, California Geological Data Map Series, Map 6, California Division of Mines and Geology, Sacramento.

Jones, L.M., Bernknopf, R., Cox, D., Goltz, J., Hudnut, K., Mileti, D., Perry, S., Ponti, D., Porter, K., Reichle, M., Seligson, H., Shoaf, K., Treiman, J., and Wein, A.,

2008, The ShakeOut Scenario: U.S. Geological Survey Open File Report 2008–1150, California Geological Survey Preliminary Report 25, version 1.0, 312 p.

Keller, E.A., Bonkowski, M.S., Korsch, R.J., and Shlemon, R.J., 1982, Tectonic Geomorphology of the San Andreas Fault Zone in the Southern Indio Hills, Coachella Valley, California: Geological Society of America Bulletin, v. 93, no. 1, p. 46-56.

Ku, T., Bull, W.B., Freeman, S.T., and Knauss, K.G., 1979, Th-230-U-234 dating of pedogenic carbonates in gravelly desert soils of Vidal Valley, southeastern California, Geological Society of America Bulletin, v. 90, p. 1063-1073.

Matmon, A., Schwartz, D.P., Finkel, R., Clemmens, S., and Hanks, T., 2005, Dating offset fans along the Mojave section of the San Andreas fault using cosmogenic Al-26 and Be-10, Geologic Society of America Bulletin, v.117, p. 795-807, doi:10.1130/B25590.

Matti, J.C., and Morton, D.M., 1993, Paleogeographic evolution of the San Andreas fault in southern California: A reconstruction based on a new cross-fault correlation, in The San Andreas Fault system: Displacement, Palinspastic Reconstruction, and Geologic Evolution, Powell, R.E., Weldon, R.J., and Matti, J.C., eds., Geol. Soc. Am. Memoir 178, 107-159.

McGill, S., Weldon, R., Kendrick, K., and Owen, L., 2006, Latest Pleistocene slip rate of the San Bernardino Strand of the San Andreas Fault in Highland; possible confirmation of the low rate suggested by geodetic data, Seismological Research Letters, v.77, no. 2, p. 279.

Meade, B.J., and Hager, B.H., 2005, Block models of crustal motion in southern California constrained by GPS measurements: Journal of Geophysical Research-Solid Earth, v. 110, no. B3, p. -.

Norris, R.M., and Webb, R.W., 1976, Geology of California, John Wiley & Sons, p. 13.

Orozco, A., 2004, Offset of a mid-holocene alluvial fan near Banning, CA: Constraints on the slip rate of the San Bernardino strand of the San Andreas Fault [M.S. thesis]: California State University, Northridge.

Philibosian, B., Fumal, T.E., Weldon, R.J., Kendrick, K.J., Scharer, K.M., Bemis, S.P., Burgette, R.J., and Wisely, B.A., 2009, Photomosaics and logs of trenches on the San Andreas Fault near Coachella, California, Open-File Report – U.S. Geological Survey.

Sieh, K.E., and Williams, P.L., 1990, Behavior of the southernmost San Andreas fault during the past 300 years, Journal of Geophysical Research, v. 95, p. 6629-6645.

Steely, A.N., Janecke, S.U., Dorsey, R.J., and Axen, G.J., 2009, Early Pleistocene initiation of the San Felipe fault zone, SW Salton Trough, during reorganization of the San Andreas fault system, GSA Bulletin, v. 121, p. 663-687.

van der Woerd, J., Klinger, Y., Sieh, K., Tapponnier, P., Ryerson, F. J., and Meriaux, A. S., 2006, Long-term slip rate of the southern San Andreas Fault from Be-10-Al-26 surface exposure dating of an offset alluvial fan: Journal of Geophysical Research-Solid Earth, v. 111, no. B4.

Weldon, R. J., II, and Sieh, K. E., 1985, Holocene rate of slip and tentative recurrence interval for large earthquakes on the San Andreas fault, Cajon Pass, southern California: Geological Society of America Bulletin, v. 96, no. 6, p. 793-812.

Yule, D., and Sieh, K., 2003, Complexities of the San Andreas fault near San Gorgonio Pass: Implications for large earthquakes: Journal of Geophysical Research, v. 108, no. B11.